European Journal of Medicinal Chemistry 92 (2015) 540–553

Contents lists available at ScienceDirect

European Journal of Medicinal Chemistry

journal homepage: http://www.elsevier.com/locate/ejmech

Original article

Design, synthesis and biological evaluation of novel 7-alkylamino substituted benzo[*a*]phenazin derivatives as dual topoisomerase I/II inhibitors

Bing-Lei Yao [1], Yan-Wen Mai [1], Shuo-Bin Chen, Hua-Ting Xie, Pei-Fen Yao, Tian-Miao Ou, Jia-Heng Tan, Hong-Gen Wang, Ding Li, Shi-Liang Huang*, Lian-Quan Gu, Zhi-Shu Huang*

School of Pharmaceutical Sciences, Sun Yat-sen University, Guangzhou 510006, People's Republic of China

ARTICLE INFO

Article history:
Received 21 December 2014
Received in revised form
10 January 2015
Accepted 11 January 2015
Available online 12 January 2015

Keywords:
Benzo[a]phenazin derivatives
Topoisomerase I
Topoisomerase II
ATPase catalytic inhibitor
Antitumor

ABSTRACT

A novel series of benzo[a]phenazin derivatives bearing alkylamino side chains were designed, synthesized and evaluated for their topoisomerases inhibitory activity as well as cytotoxicity against four human cancer cell lines (HL-60, K-562, HeLa, and A549). These compounds were found to be dual inhibitors of topoisomerase (Topo) I and Topo II, and exhibited excellent antiproliferative activity, in particular against HL-60 cells with submicromolar IC_{50} values. Further mechanistic studies showed that this class of compounds acted as Topo I poisons by stabilizing the Topo I-DNA cleavage complexes and Topo II catalytic inhibitors by inhibiting the ATPase activity of *h*Topo II. Molecular docking studies revealed the binding modes of these compounds for Topo I and Topo II.

1. Introduction

Topoisomerases are nuclear enzymes that modulate the topological state of DNA during various key cellular processes such as replication, transcription, recombination, repair, and chromatin assembly [1–4]. Topoisomerases have been recognized as one of the most promising targets in anticancer drug discovery because of their highly over-expression in cancer cells [5]. There are two major classes of topoisomerases, namely, topoisomerase type I (Topo I) and type II (Topo II). Topo I catalyzes the formation of DNA single-strand breaks while Topo II engenders DNA double-strand breaks [6–8]. On the basis of their mechanism of action, Topo inhibitors are classified into two categories, Topo poisons, which interfere with the breaking–rejoining reaction of the enzyme by stabilizing the cleavable complex of Topo with DNA, and catalytic inhibitors that impair Topo activity without stabilizing the cleavable complex and act at any one of several steps within the Topo catalytic cycle [9–11].

Drugs that specifically target Topo I, principally the camptothecin analogs, have made an important impact more recently for the treatment of colon cancer [12], while those that target Topo II, for example etoposide and doxorubicin, have been used for treatment of a wide variety of malignancies [13]. Since both Topo I and Topo II are excellent targets, it would be desirable to jointly inhibit them. In this regard, a single compound able to inhibit both Topo I and II appears to combine the properties of the individual specific inhibitor, thus leading to a more promising anti-tumor activity [3]. A number of drugs such as the acridine DACA [14], the benzophenazine XR11576 [12], the benzopyridoindole intoplicine [15], the indenoquinolinone TAS-103 [16], the pyrazoloacridine NSC 366140 [17], and the tafluposide (F-11782) [18], have now been identified to target both Topo I and Topo II simultaneously, and some of these drugs have been advanced to clinical trial [19].

Benzophenazine derivatives are considered to be potentially bioactive compounds. NC-190 is an anti-tumor compound having a benzo[*a*]phenazine ring and displays strong Topo II inhibition and weak Topo I inhibition. Further studies have revealed NC-190 could induce Topo II-mediated DNA cleavage and DNA fragmentation in

* Corresponding authors.
E-mail addresses: lsshsl@mail.sysu.edu.cn (S.-L. Huang), ceshzs@mail.sysu.edu.cn (Z.-S. Huang).
[1] These authors contributed equally.

http://dx.doi.org/10.1016/j.ejmech.2015.01.024
0223-5234/

Abbreviations

CPT	camptothecin
EB	ethidium bromide
HPLC	high performance liquid chromatography
HRMS	high resolution mass spectrometer
MTT	methyl thiazolyl tetrazolium
NMR	nuclear magnetic resonance
1,4-NQ	1,4-naphthoquinone
SARs	structure–activity relationship
Topo	topoisomerase
Topo I	topoisomerase type I
Topo II	topoisomerase type II
VP-16	etoposide

HL-60 cells [20,21]. Similarly, XR 11576, a lipophilic benzo[*a*]phenazine developed by Xenova and Millennium, has been proved to be a potent dual inhibitor of Topo I and II, inducing cleavage of complex formed by both Topo I and Topo II as dual poison at low concentrations [19,22,23].

To discover novel anticancer agent as dual Topo inhibitors, we have previously reported the modification strategy on ring B and ring D of the benzo[*a*]phenazine scaffold and successfully developed compound **5d-1** which has been proved to be a rare dual Topo inhibitors by acting as Topo I poisons and Topo II catalytic inhibitors [24]. In an effort to gain more insight into the substitution effects on ring A, ring C and ring D and make change from phenolic ether form to quinone imide form, we synthesized a series of benzo[*a*]phenazin derivatives by attaching alkylamino side chains to the nitrogen group on ring C with or without different substitutive group on ring A and ring D (Fig. 1).

In this study we report the design and synthesis of benzo[*a*]phenazin derivatives and evaluation of their Topo I and II inhibitory activity, and cytotoxicity against four human cancer cell lines. To further investigate the action mechanism of these compounds, several *in vitro* experiments including cleavage complex assays and ATPase activity assays were performed. Our results indicated that this type of compounds were dual Topo inhibitors by acting as Topo I poisons and Topo II catalytic inhibitors.

2. Chemistry

The designed compounds were synthesized by following existing procedures with modifications [25], as shown in Scheme 1. Treatment of 2-fluoro-nitrobenzene (**1a**, **1e-1** ~ **1e-3**) or 2-chloro-3-nitropyridine (**1g**) with the appropriate diamines in the presence of tetrahydrofuran afforded the intermediates **2**. The nitro group of intermediates **2** was reduced to amines to provide the corresponding intermediates **3** by using Zn/acetic acid as a reducing agent. In the presence of potassium *tert*-butoxide, 2-hydroxy-1,4-naphthoquinone derivatives **5** (**5a**, **5b**) were readily prepared by autoxidation of methoxyl tetralones **4** (**4a**, **4b**). 2-Hydroxy-1,4-naphthoquinone anologs **5** and intermediates **3** were condensed in acetic acid for 60 min at 60 °C to give benzo[*a*]phenazin derivatives **6**. All structures of compounds **6** were confirmed using ^{1}H NMR, ^{13}C NMR and HRMS (ESI).

3. Results and discussion

3.1. Topo I and II inhibitory activity

Topo I and II Inhibitory activity was measured by detecting the conversion of supercoiled pBR322 plasmid DNA to its relaxed form in the presence of the tested compounds as shown in Figs. 2 and 3. Camptothecin and etoposide, well known Topo I and II inhibitors, respectively, were used as positive controls. As shown in Fig. 2A, most of compounds showed good Topo I inhibitory activity at 50 μM concentration, and compounds **6c-1**, **6d-4**, and **6e-3** showed significant Topo I inhibitory activity in further screening assay at 25 μM concentrations (Fig. 2B).

The results of Topo I inhibitory activities indicated that introduction of the terminal amino moiety into the side chain at *N-7* position of benzo[a]phenazine scaffold could increase the inhibitory activity of the compounds compared to the compound **6a-6** without terminal amino moiety. Those compounds with the dimethylamino terminal (**6a-1**, **6b-1**, **6c-1**) of the side chain at *N-7* position showed good inhibitory activity. Comparing the activity of three series compounds **6a-1** ~ **6a-6** (n = 1), **6b-1** ~ **6b-6** (n = 2) and **6c-1** ~ **6c-2** (n = 3), it could be found that the activities of these tested compounds were not affected by the length of the side chains. By comparing with **6b-1** at inhibitory concentration of 25 μM (Fig. 2B), we could find that the introduction of $-OCH_3$

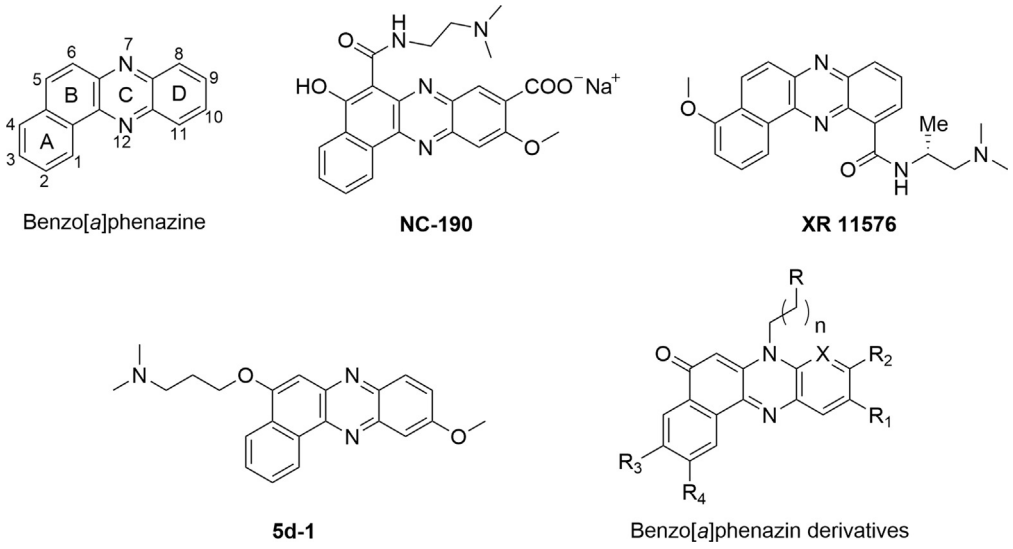

Fig. 1. Structure of benzophenazine derivatives.

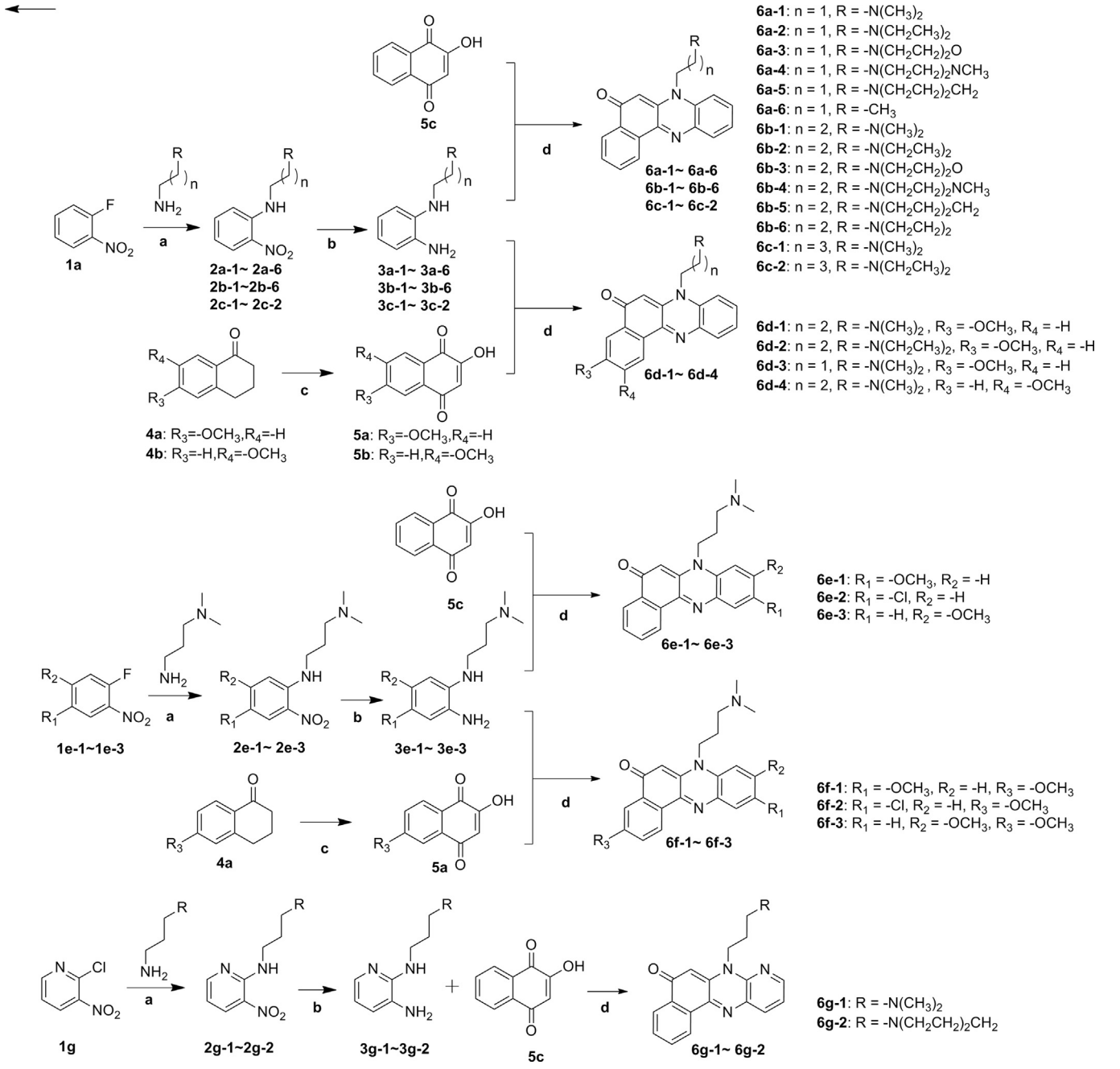

Scheme 1. Syntheses of benzo[a]phenazin derivatives. Reagents and conditions: (a) THF, 30 °C, 12 h; (b) AcOH, Zn, 0 °C, 1 h; (c) *t*-BuOK, *t*-BuOH, O_2, 2 h, 42%-45%; (d) AcOH, 60 °C, 1 h, 41% ~ 48%.

groups at position of C-2 (**6d-4**) or C-9 (**6e-3**) increased the inhibitory activity of the tested compounds, while other substitution patterns did not produce favorable effects on inhibitory activity.

The effect of the tested compounds on human DNA Topo II was shown in Fig. 3. Most of the compounds showed good Topo II inhibitory activity at 50 μM concentrations except compounds **6a-2**, **6a-3**, **6a-6**, **6d-2**, **6d-3**, and **6f-2** (Fig. 3A). Further screening assay showed that compounds **6c-1**, **6d-4**, and **6f-3** could inhibit completely Topo II at 25 μM concentration (Fig. 3B).

The structure–activity relationship (SARs) analysis on Topo II was similar to that on Topo I. The results indicated that the terminal amino moiety is important for inhibitory activity, as compound **6a-6** had lower activity against Topo II. Compounds with the dimethylamino terminal (**6a-1**, **6b-1**, **6c-1**) and piperidine terminal (**6a-5**, **6b-5**) side chain at *N-7* position exhibited significant inhibitory activity and the length of side chain was not important to inhibitory activity. Compound **6d-4** with $-OCH_3$ group at position C-2 showed both good Topo I and Topo II inhibitory activity at 25 μM. Additionally, compound **6f-3** with $-OCH_3$ group at the position C-3 and C-9 displayed good Topo II inhibitory activity at 25 μM. Moreover, compounds **6g-1** and **6g-2**, which possess *N* at 8 position of ring D of benzo[*a*]phenazine scaffold, did not show significant Topo I and Topo II inhibitory activity at 25 μM, indicating that the inhibitory activities of the test compounds were not affected by the introduction of *N* into 8 position of ring D of benzo [*a*]phenazine scaffold.

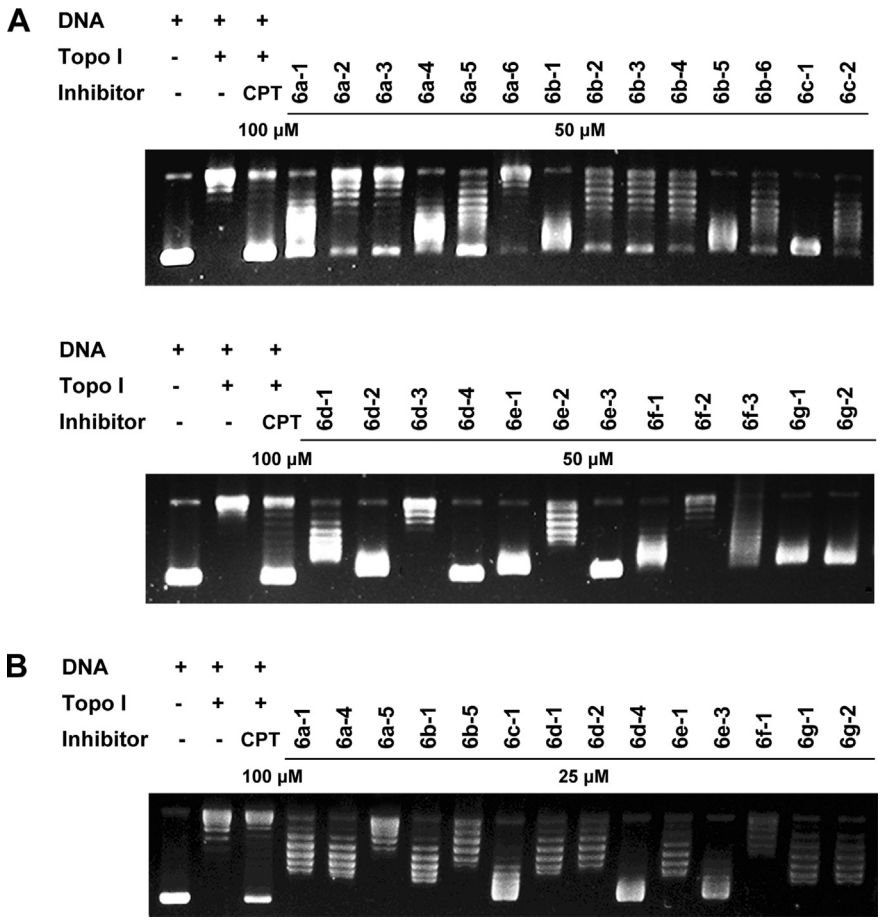

Fig. 2. The Topo I inhibitory activity of benzo[a]phenazine derivatives. Supercoiled pBR322 plasmid was incubated with Topo I in the presence or absence of indicated compounds at 37 °C for 30 min. (A) Effect of **6a-1** ~ **6a-6**, **6b-1** ~ **6b-6**, **6c-1** ~ **6c-2**, **6d-1** ~ **6d-4**, **6e-1** ~ **6e-3**, **6f-1** ~ **6f-3**, and **6g-1** ~ **6g-2** on DNA relaxation catalyzed by Topo I at the concentration of 50 μM. (B) Effect of **6a-1**, **6a-4**, **6a-5**, **6b-1**, **6b-5**, **6c-1**, **6d-1**, **6d-2**, **6d-4**, **6e-1**, **6e-3**, **6f-1**, **6g-1**, and **6g-2** on DNA relaxation catalyzed by Topo I at the concentration of 25 μM.

3.2. Cytotoxicity

The synthesized compounds were evaluated for their cytotoxic activities against four cancer cell lines including HL-60 (human myeloid leukemic tumor cell line), K562 (human myeloid leukemic tumor cell line), HeLa (human cervix tumor cell line) and A549 (adenocarcinomic human alveolar basal epithelial cell line) using the MTT [3-(4,5-dimethylthiazol-2-yl)-2,5-diphenyl-2H-tetrazolium bromide] assay as described by Mosmann with modifications [26]. Camptothecin (CPT) and etoposide (VP-16) were used as positive controls. The inhibitory activities (IC_{50}) of the tested compounds are shown in Table 1.

From the IC_{50} values, it is clear that most compounds were more sensitive against HL-60 cell line than against other three cell lines. This result is consistent with that observed for the positive controls. For HL-60 cell line, twenty compounds displayed potent inhibitory activities with the IC_{50} values range from 0.09 μM to 0.96 μM. Among these compounds, eleven compounds for A549 cell line, five compounds for HeLa cell line, and only one compound for K562 cell line showed better inhibitory activities than positive control CPT. Base on the MTT data of sensitive cell HL-60, the cytotoxicity of compounds were not affected by length of side chain. Compounds **6a-1** (n = 1), **6b-1** (n = 2), and **6c-1** (n = 3) have similar cytotoxic activity. In addition, the terminal amino moiety of side chain is important for their cytotoxicity. For example, **6a-6**, without terminal amino moiety hardly possessed any cytotoxicity for four cancer cell lines. The morphorine substituent in terminal amino moiety and 10-Cl substituent at D ring decreased their cytotoxicity. For example, **6e-2** (IC_{50} = 1.08 μM) and **6f-2** (IC_{50} = 6.43 μM) had decreased activity compare with the corresponding compounds **6b-1** (IC_{50} = 0.21 μM) and **6d-1** (IC_{50} = 0.15 μM).

To some extent, the SARs have shown some correlation between the cytotoxicity and Topo inhibitory activity. The compounds without Topo I and Topo II inhibitory activity at 25 μM concentration also exhibited low cytotoxicity (The IC_{50} values for **6a-3**, **6a-6**, **6b-2** ~ **4**, **6d-3**, **6e-2**, **6f-2** were all more than 1.0 μM for HL-60 cell line). Although compounds **6c-1** and **6d-4** displayed the highest Topo I and II inhibitory activity, they were not the most potent compounds in cytotoxicity against HL-60 cell line. In addition, compounds **6a-2**, **6c-2**, and **6d-1** which showed moderate or weak Topo inhibition, also possessed potent cytotoxicity against HL-60 cell line. Therefore, for most of the compounds, this might be due to different expression levels of Topo I and II in the tested cell lines and the diverse mechanisms in inhibiting human Topo I and II [27].

3.3. Topo I-mediated DNA cleavage assay

The results of Topo I mediated DNA relaxation assays suggested that Topo I is a target for our compounds. With the aim to further understand the mechanism of action of our compounds, we performed the Topo I cleavage assay to see if our compounds can act as Topo I poisons by stabilizing the Topo I-DNA cleavage complexes.

Compound **6c-1** was chosen to evaluate the occurrence of the cleavage complexes by the induction of nicked DNA. Camptothecin,

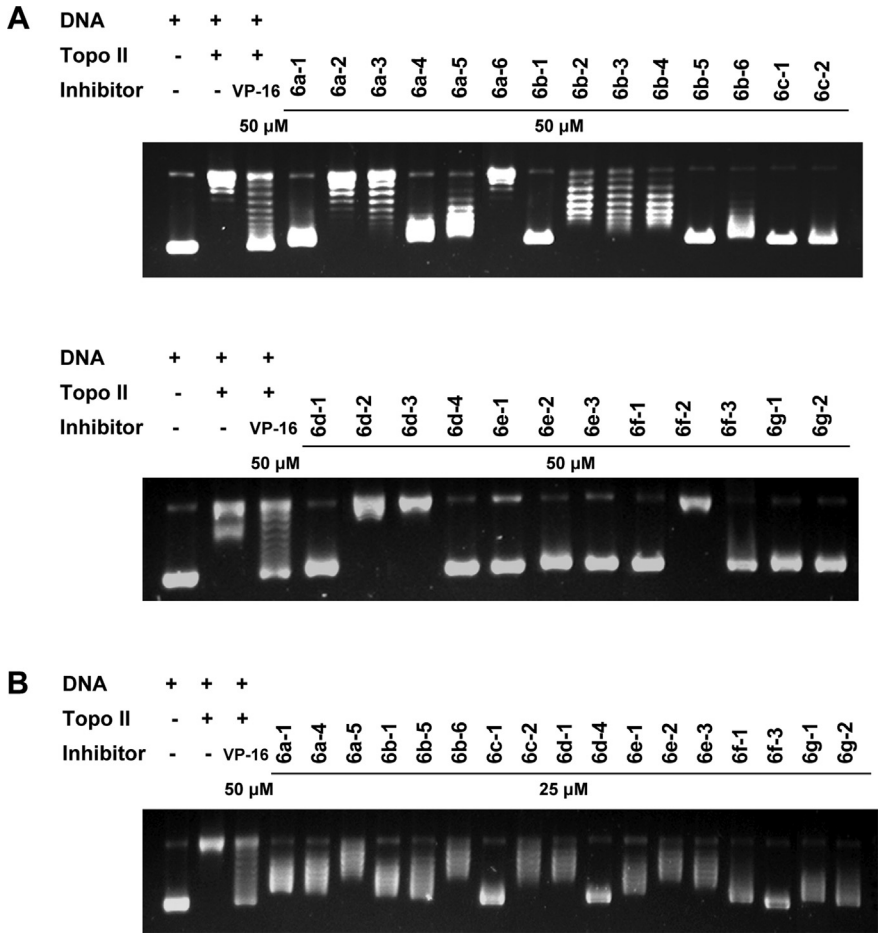

Fig. 3. The Topo II inhibitory activity of benzo[a]phenazine derivatives. Supercoiled pBR322 plasmid was incubated with Topo II in the presence or absence of indicated compounds at 37 °C for 30 min. (A) Effect of **6a-1** ~ **6a-6**, **6b-1** ~ **6b-6**, **6c-1** ~ **6c-2**, **6d-1** ~ **6d-4**, **6e-1** ~ **6e-3**, **6f-1** ~ **6f-3**, and **6g-1** ~ **6g-2** on DNA relaxation catalyzed by Topo II at concentration of 50 μM. (B) Effect of **6a-1**, **6a-4**, **6a-5**, **6b-1**, **6b-5**, **6b-6**, **6c-1**, **6c-2**, **6d-1**, **6d-4**, **6e-1**, **6e-2**, **6e-3**, **6f-1**, **6f-3**, **6g-1**, and **6g-2** on DNA relaxation catalyzed by Topo II at concentration of 25 μM.

a well-known Topo I poison, was used as positive control. As shown in Fig. 4A, both **6c-1** and CPT could stabilize the cleavage complex by inducing the formation of nicked DNA. Analysis of optical density of the nicked DNA induced by CPT revealed that CPT could stabilize the cleavage complex in a dose-dependent manner. As shown in Fig. 4B, the amount of nicked DNA increased significantly with increasing concentrations of camptothecin. By comparison, although compound **6c-1** could induce the formation of nicked DNA but the amount of nicked DNA increased with increasing concentrations of **6c-1** at lower concentration (0.5–10 μM) was not as obviously as that of CPT. **6c-1** exhibited its maximal cleavage enhancement at 10 μM by increasing the amount of nicked DNA of 2.5 fold and showed a decline of nicked DNA at higher concentration (25–50 μM). The lower concentration of **6c-1** producing a weakly increase of nicked DNA and the higher concentration of **6c-1** leading to a gradually decrease of nicked DNA might be because the intercalative ability of compound hampered the interaction between Topo I and DNA [28].

To examine if our compound could induce the formation of Topo I-DNA cleavage complexes *in vivo*, we further performed the ICE (immunodetection of complexes of enzyme-to-DNA) assay. As shown in Fig. 4C, after the exposure to our compounds for 1 h, both CPT and the selected compound **6c-1** induced the formation of Topo I-DNA cleavage complexes in a dose-dependent manner at lower concentration. These results were consistent with those of *in vitro* experiment indicating that our compounds act as Topo I poisons by trapping Topo I-DNA cleavage complexes.

3.4. Topo II-mediated DNA cleavage assay

Similar to Topo I, our compounds showed good inhibition against relaxation activity of Topo II. In order to investigate the mode of action of our compounds, Topo II-mediated cleavage assays were performed to differentiate Topo II poisons and catalytic inhibitors based on whether or not linear DNA is formed.

Compound **6c-1** was chosen to test for its ability to induce the formation of linear DNA in Topo II-mediated DNA cleavage assays. In this assay, VP-16 was chosen as a positive control. As shown in Fig. 5, VP-16 induced the formation of linear DNA, in contrast, treatment with compound **6c-1** did not generate any linear DNA at 10 and 50 μM, thus indicating its inability to induce the formation of cleavage complex. Based on these observations, it is possible to deduce that compound **6c-1** might not be a Topo II poison but a catalytic inhibitor.

3.5. ATPase domain of hTopo II related assays

In order to investigate the interaction between our compounds and the ATPase domain of Topo II, we examined the effect of our compounds on the ATPase activity to see if our compounds can

Table 1
IC_{50} values (μM) of the benzo[a]phenazin derivatives against cancer cells.

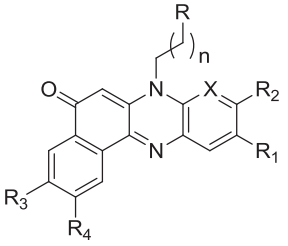

6a-1~6a-6, 6b-1~6b-6, 6c-1~6c-2, 6d-1~6d-4, 6e-1~6e-3, 6f-1~6f-3, 6g-1~6g-2

Compd.	n	R	R_1	R_2	R_3	R_4	X	IC_{50} (μM)[a]			
								HL-60	K562	Hela	A549
6a-1	1	$-N(CH_3)_2$	−H	−H	−H	−H	−C	0.31	24.56	9.91	22.31
6a-2	1	$-N(CH_2CH_3)_2$	−H	−H	−H	−H	−C	0.31	25.57	25.45	29.24
6a-3	1	$-N(CH_2CH_2)_2O$	−H	−H	−H	−H	−C	6.91	>40	>50	>50
6a-4	1	$-N(CH_2CH_2)_2NCH_3$	−H	−H	−H	−H	−C	0.38	21.56	28.95	25.26
6a-5	1	$-N(CH_2CH_2)_2CH_2$	−H	−H	−H	−H	−C	0.93	25.17	31.96	37.31
6a-6	1	$-CH_3$	−H	−H	−H	−H	−C	32.12	>40	>50	>50
6b-1	2	$-N(CH_3)_2$	−H	−H	−H	−H	−C	0.21	5.93	8.41	13.51
6b-2	2	$-N(CH_2CH_3)_2$	−H	−H	−H	−H	−C	1.50	24.76	44.48	37.41
6b-3	2	$-N(CH_2CH_2)_2O$	−H	−H	−H	−H	−C	1.28	25.17	>50	45.35
6b-4	2	$-N(CH_2CH_2)_2NCH_3$	−H	−H	−H	−H	−C	1.22	23.96	26.74	23.57
6b-5	2	$-N(CH_2CH_2)_2CH_2$	−H	−H	−H	−H	−C	0.52	10.34	27.45	32.96
6b-6	2	$-N(CH_2CH_2)_2$	−H	−H	−H	−H	−C	0.22	25.17	30.26	35.68
6c-1	3	$-N(CH_3)_2$	−H	−H	−H	−H	−C	0.38	4.73	21.44	16.28
6c-2	3	$-N(CH_2CH_3)_2$	−H	−H	−H	−H	−C	0.22	25.97	29.45	18.85
6d-1	2	$-N(CH_3)_2$	−H	−H	$-OCH_3$	−H	−C	0.15	6.12	28.38	24.56
6d-2	2	$-N(CH_2CH_3)_2$	−H	−H	$-OCH_3$	−H	−C	0.23	21.96	25.95	22.94
6d-3	1	$-N(CH_3)_2$	−H	−H	$-OCH_3$	−H	−C	2.85	18.35	18.93	38.47
6d-4	2	$-N(CH_3)_2$	−H	−H	−H	$-OCH_3$	−C	0.22	7.13	29.95	32.96
6e-1	2	$-N(CH_3)_2$	$-OCH_3$	−H	−H	−H	−C	0.96	20.16	24.94	25.95
6e-2	2	$-N(CH_3)_2$	−Cl	−H	−H	−H	−C	1.08	20.36	29.56	38.41
6e-3	2	$-N(CH_3)_2$	−H	$-OCH_3$	−H	−H	−C	0.18	5.53	5.51	30.46
6f-1	2	$-N(CH_3)_2$	$-OCH_3$	−H	$-OCH_3$	−H	−C	0.65	21.96	6.52	34.46
6f-2	2	$-N(CH_3)_2$	−Cl	−H	$-OCH_3$	−H	−C	6.43	22.76	42.98	31.46
6f-3	2	$-N(CH_3)_2$	−H	$-OCH_3$	$-OCH_3$	−H	−C	0.09	8.73	18.23	26.45
6g-1	2	$-N(CH_3)_2$	−H	−H	−H	−H	−N	0.62	36.79	4.52	20.44
6g-2	2	$-N(CH_2CH_2)_2CH_2$	−H	−H	−H	−H	−N	0.63	38.39	20.44	19.93
VP-16	–	–	–	–	–	–	–	0.06	1.64	0.54	8.91
CPT	–	–	–	–	–	–	–	0.07	5.37	11.62	26.45

[a] The IC_{50} represents compound concentration giving 50% survival of each cell line.

inhibit ATP hydrolysis. As shown in Fig. 6A, all of the selected compounds with significant Topo II inhibitory activity at 25 μM, showed good inhibitory activities higher than the positive control 1,4-naphthoquinone (1,4-NQ) [29]. Especially, compounds **6f-3** showed the best inhibitory activity of 78% on ATP hydrolysis, comparing with 56% for 1,4-NQ.

To further determine the mode of action for this class of compounds towards ATPase of *h*Topo II, an *in vitro* DNA independent ATP hydrolysis assay was performed using compound **6f-3**. Different concentrations of ATP (0.25, 0.5, 0.8, 1.0, and 2.0 mM) were incubated with compound **6f-3** of a fixed concentration at 0, 5, 25, 50, and 100 μM, respectively. As shown in Fig. 6B, compound **6f-3** effectively inhibited ATPase of *h*Topo II in a concentration-dependent manner. The double reciprocal Lineweaver–Burk plot revealed a decrease in K_m while no change in V_{max}. This result indicated that compound **6f-3** acted as a competitive inhibitor of ATP.

3.6. DNA-binding properties

Since the DNA intercalators can interfere with the DNA relaxation reaction by altering the apparent topological state of negatively supercoiled DNA substrate, they induce constrained negative and unstrained positive superhelical twists in plasmids DNA [16]. We performed the DNA unwinding assay by using eukaryotic DNA Topo I to clarify the intercalation property of the compounds. In the presence of the DNA intercalators, a relaxed plasmid DNA appears to be supercoiled plasmid DNA by treatment with Topo I. As shown in Fig. 7A, ethidium bromide (EB), a well-known DNA intercalator, intercalated into plasmid DNA by converting relaxed DNA to supercoiled DNA substrate in the presence of Topo I in dose-dependent manner. In the presence of the selected compound **6c-1**, relaxed DNA was transformed into supercoiled DNA substrate by treatment with Topo I, which was identical to the action of ethidium bromide (EB). This finding provided evidence that compound **6c-1** could intercalate into DNA. However, the ability of compound **6c-1** to intercalate into DNA was far less than that of EB, and had less Topo I/II inhibitory activity and cytotoxicity towards cancer cell lines.

The intercalating ability of the compounds was also assessed by using UV–Vis spectrometry characterization of the compounds in absence or presence of CT-DNA. It is widely accepted that if the compounds could intercalate into DNA, the UV–Vis curve of their complex would demonstrate hypochromicity and bathochromic shifts [30]. As shown in Fig. 7B, when increasing the concentration of DNA, the absorption spectra of compound **6c-1** showed a significant hypochromicity but without an obvious bathochromic shift, indicating that compound **6c-1** had a strong interaction with

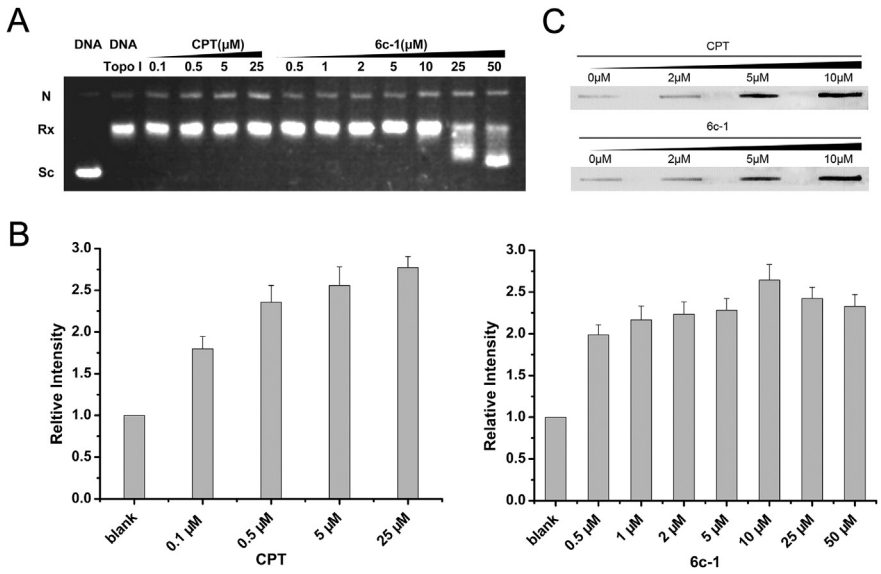

Fig. 4. (A) Effects of CPT and **6c-1** on Topo I-DNA cleavage complexes formation at various concentrations. Agarose gel electrophoresis of pBR322 (0.1 μg) DNA containing increasing concentration of CPT and **6c-1** upon treatment with excess Topo I (10 units). (B) Optical density analysis of the nicked DNA induced by CPT and **6c-1** at various concentrations. (C) Analysis of cellular Topo I-DNA cleavage complexes induced by CPT and **6c-1** at concentrations of 2, 5 and 10 μM, respectively. 0 μM represents the blank control group (upper) and 1.0% DMSO (v/v) control group (bottom).

DNA. The further analysis of the results revealed the K_{app} value of compound **6c-1** and DNA was 4.83×10^5 M^{-1}.

3.7. Molecular modeling

Since the mechanism studies revealed that this class of compounds could stabilize the Topo I-DNA cleavage complexes and inhibit the ATPase activity of Topo II, molecular docking stimulations were performed to better understand the potential interaction mode of these compounds with the Topo I-DNA cleavage complexes (PDB code: 1K4T) and the ATPase domain of Topo II (PDB code: 1ZXM), respectively.

Compound **6c-1** was chosen to simulate the interaction with the Topo I-DNA cleavage complexes. As shown in Fig. 8A, it was found that **6c-1** was well-fitted into the site of DNA cleavage and formed base-stacking interactions with both the −1 (upstream) and +1 (downstream) base pairs of DNA. Besides, the nitrogen cation of side chain formed hydrogen bonding interaction with TGP 11 and had electrostatic interaction with the carboxyl group of Asp533. The interaction mode of the selected compound **6f-3** with the ATPase domain of Topo II was also explored as shown in Fig. 8B. Compound **6f-3** was docked into the ATP binding site of the ATPase domain of Topo II. It was found that **6f-3** could fit into the ATP binding pocket, and form hydrophobic interaction with Ile141, Val137, Phe142, Pro126, Ile125, and Asn91. In addition, the positive charge on nitrogen of side chain formed hydrogen bonding interaction with Thr147. Moreover, the carbonyl group at C-5 position of ring B of benzo[*a*]phenazin scaffold was close to Ser148 and Ser149, indicating that it may have the potential to form hydrogen bonding interaction with these two amino acid residues. The docking results further confirmed the importance of the terminal amino side chain in inhibitory activity against Topo I and II.

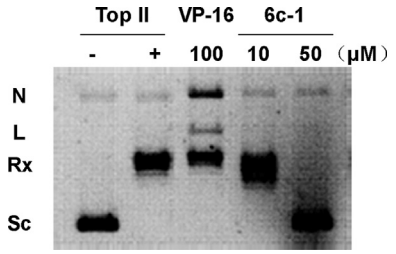

Fig. 5. Topo II mediated cleavage assay of plasmid pBR322 DNA. Lane 1: pBR322 DNA only. Lane 2: pBR322 DNA and Topo II. Lane 3: 100 μM VP-16, Topo II and pBR322 DNA. Lane 4–5: **6c-1** (10 μM, 50 μM), Topo II and pBR322 DNA.

4. Conclusion

In this paper, a series of novel benzo[*a*]phenazin derivatives were designed, synthesized and evaluated for Topo I and II inhibitory activity and cytotoxicity against several human cancer cell lines. Some of the compounds exhibited significant Topo I and Topo II inhibitory activity at 25 μM concentration. Our MTT assays showed that most of these compounds had better activity for HL-60 cells than the other three tested cell lines, with IC_{50} values in the submicromolar range. The cytotoxicity of these compounds had some relationship with their Topo I and II inhibitory activity. Investigation of SARs revealed that the substitution of amino groups on terminal of side chain at *N*-7 position could significantly enhance the Topo I and II inhibitory activity and cytotoxicity of the compounds. Among these compounds, the compounds with the dimethylamino terminal (**6a-1**, **6b-1**, **6c-1**) showed good Topo I and Topo II inhibitory activity while the compounds with other terminal groups exhibited partial or moderate inhibition of Topo I and Topo II. Our results indicated that the type of terminal amino moiety had a crucial role in the inhibitory activity. Introduction of different substitutive group on the ring A or ring D of the scaffolds did not produce favorable effects on Topo I and Topo II activity. Only compound **6d-4** with $-OCH_3$ group at position C-9 exhibited good Topo I and Topo II inhibitory activity at 25 μM concentration. Further mechanistic studies showed that this class of compounds could stabilize the Topo I-DNA cleavage complexes and inhibit the ATPase activity of *h*Topo II, indicating that these compounds are dual Topo inhibitors by functioning as Topo I poisons and Topo II catalytic inhibitors. The ICE assay further demonstrated **6c-1** could stabilize the Topo I-DNA cleavage complexes *in vivo*, and kinetic studies revealed that **6f-3** acted as a competitive inhibitor of ATP. Molecular docking studies

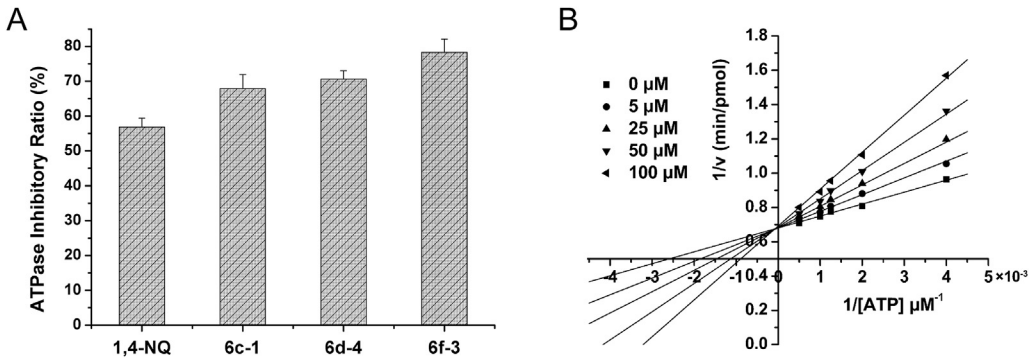

Fig. 6. (A) ATPase inhibitory activity of **6c-1**, **6d-4**, and **6f-3** in the presence of 1 mM ATP. The inhibition of ATPase activity was measured by adding 1 mM of each compound to the reaction at final concentration of 100 μM. The optical density (OD_{620}) values obtained for the compounds were compared against the background group without enzyme, which was set as 100% inhibitory rate, while the enzyme only group was set as 0% inhibitory rate. (B) The double reciprocal Lineweaver–Burk plot for ATP-hydrolysis activity of ATPase in the absence of DNA.

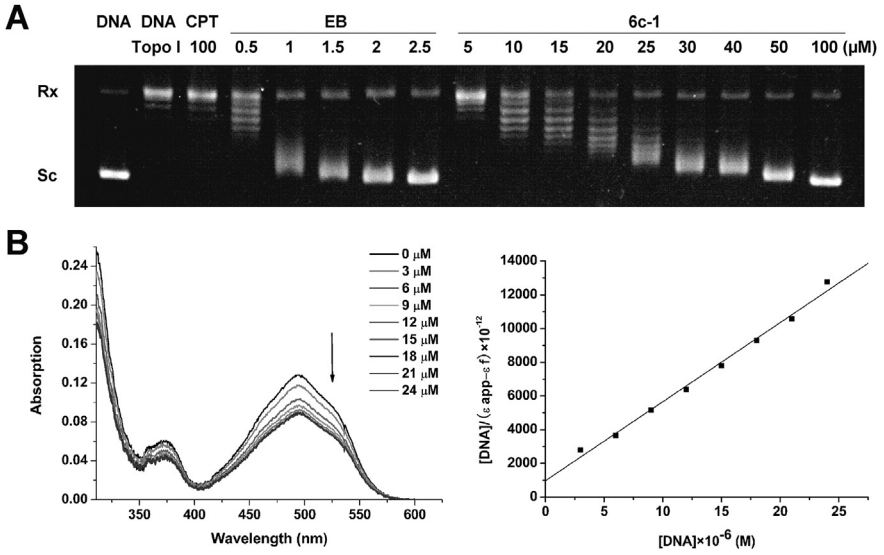

Fig. 7. Effect of **6c-1** on DNA unwinding. (A) Agarose gel electrophoresis of relaxed pBR322 DNA containing increasing concentration of EB and **6c-1**. (B) Absorption spectra of **6c-1** upon addition of CT-DNA. [**6c-1**] = 15 μM, [DNA] = 0–24 μM. Arrow indicated the absorption change upon increasing amount of CT-DNA. Insert graph shows the plot of [DNA]/($\varepsilon_a-\varepsilon_f$) versus [DNA].

suggested that these novel compounds exerted their Topo I and Topo II inhibitory activity via intercalating into the cleavage site of the Topo I-DNA cleavage complexes and blocking the ATP-binding site of Topo II, respectively. Our present results could provide useful information for further structural modification of benzophenazin for discovery of potent anticancer drugs.

5. Experimental section

5.1. Chemistry

All commercial chemicals used as starting materials were analytical grade and utilized without further purification. Melting

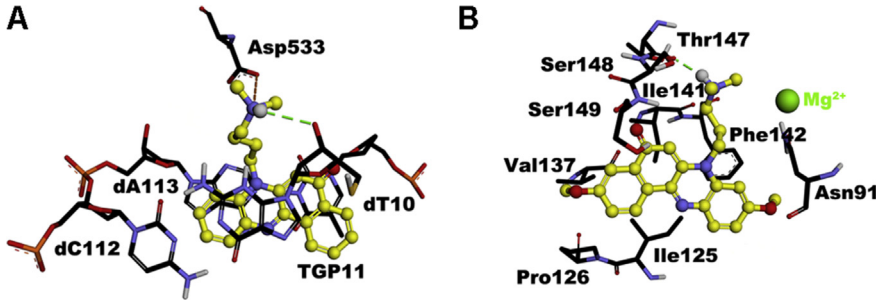

Fig. 8. Results of the docking simulation for compounds **6c-1** and **6f-3**. (A) Binding mode of **6c-1** with Topo I-DNA complex. (B) Binding mode of **6f-3** with ATPase binding site of Topo II. The green dashed lines indicate the hydrogen bonding interaction, and the red dashed lines represent the electrostatic interaction. (For interpretation of the references to colour in this figure legend, the reader is referred to the web version of this article.)

points were determined by using capillary tubes with a MSRS-OptiMelt Automated Melting point system and are uncorrected. ^{1}H and ^{13}C NMR spectra were recorded using TMS as the internal standard in $CDCl_3$, D_2O, DMSO-d_6 or CD_3OD with a Bruker BioSpin GmbH spectrometer at 400 MHz. High resolution mass spectra (HRMS) were recorded on Shimadzu LCMS-IT-TOF. The purity of synthesized compounds was proved to be more than 95% by using analytical HPLC equipped with Shimadzu LC-20AB system and an Ultimate XB-C18 column (4.6 × 250 mm, 5 μm), which was eluted with methanol–water (70:30–90:10) containing 0.1% TFA at a flow rate of 0.2 mL/min.

*5.1.1. General procedure for the preparation of intermediate **2a-1 ~ 2a-6**, **2b-1 ~ 2b-6**, **2c-1 ~ 2c-2**, **2e-1 ~ 2e-3**, **2g-1 ~ 2g-2***

Compound **1** (20 mmol) and proper amine (20 mmol) were dissolved in tetrahydrofuran, and the reaction mixture was stirred at 30 °C for 12 h under nitrogen. After completion of the reaction, the mixture was then extracted with dichloromethane after evaporating the tetrahydrofuran, washed with water, and concentrated to provide crude oil product. The residue was used for next synthetic step without further purification.

*5.1.2. General procedure for the preparation of intermediates **3a-1 ~ 3a-6**, **3b-1 ~ 3b-6**, **3c-1 ~ 3c-2**, **3e-1 ~ 3e-3**, **3g-1 ~ 3g-2***

Above intermediate **2** was dissolved in 100 mL acetic acid, and cooled in ice bath. 100 mmol of Zinc powder was added to the solvent slowly in three portions over 30 min. The reaction mixture was warmed to room temperature and stirred for another 30 min. After the reaction was completed, the mixture was filtered and filtrate was used for next step without further purification.

*5.1.3. General procedure for the preparation of intermediates **5a** and **5b***

A solution of compound **4** (20 mmol) in dry *t*-BuOH (50 mL) was added to a 1 M solution of KO-*t*-Bu in dry *t*-BuOH (50 mL) which had previously been saturated with O_2 and the red solution vigorously stirred in an atmosphere of O_2 until 2 equiv were absorbed. After the reaction was completed, the cooled solution was acidified with concentrated HCl, and yellow precipitate was formed immediately. Then the reaction mixture was filtered and the precipitate was washed with water, dried over anhydrous sodium sulfate, and concentrated to give the desired product [31,32].

*5.1.3.1. 2-Hydroxy-6-methoxynaphthalene-1,4-dione (**5a**).* Yellow solid, yield 45.2%. ^{1}H NMR (400 MHz, $CDCl_3$) δ 8.06 (d, *J* = 8.4 Hz, 1H), 7.57 (s, 1H), 7.43 (s, 1H), 7.16 (d, *J* = 6.3 Hz, 1H), 6.30 (s, 1H), 3.97 (s, 3H).

*5.1.3.2. 2-Hydroxy-7-methoxynaphthalene-1,4-dione (**5b**).* Yellow solid, yield 42.7%. ^{1}H NMR (400 MHz, DMSO-d_6) δ 7.88 (d, *J* = 8.6 Hz, 1H), 7.41 (d, *J* = 2.6 Hz, 1H), 7.35 (dd, *J* = 8.6, 2.7 Hz, 1H), 6.14 (s, 1H), 3.92 (s, 3H).

*5.1.4. General procedure for the preparation of **6a-1 ~ 6a-6**, **6b-1 ~ 6b-6**, **6c-1 ~ 6c-2**, **6d-1 ~ 6d-4**, **6e-1 ~ 6e-3**, **6f-1 ~ 6f-4**, and **6g-1 ~ 6g-2***

To a stirred solution of above intermediates **3** in 100 mL acetic acid, 2-hydroxy-1,4-naphoquinone anologs **5** (20 mmol) was added at room temperature. Precipitate was formed immediately. Stirring was continued for 60 min at 60 °C. Then, the mixture was filtered and the precipitate was washed with water to give crude solid product. The solid residue was purified by using chromatography with PE/CH_2Cl_2/MeOH/$NH_3 \cdot H_2O$ elution to give the desired product [25].

*5.1.4.1. 7-(2-(Dimethylamino)ethyl)benzo[a]phenazin-5(7H)-one (**6a-1**).* Red solid, yield 47.2%. m.p. 168.4–171.3 °C. ^{1}H NMR (400 MHz, DMSO-d_6) δ 8.84 (d, *J* = 6.7 Hz, 1H), 8.21 (d, *J* = 5.7 Hz, 1H), 8.01 (d, *J* = 7.4 Hz, 1H), 7.89–7.69 (m, 4H), 7.49 (t, *J* = 7.2 Hz, 1H), 6.18 (s, 1H), 4.44 (s, 2H), 2.71 (s, 2H), 2.34 (s, 6H). ^{13}C NMR (101 MHz, MeOD) δ 183.1, 146.4, 140.3, 136.2, 133.3, 132.9, 132.1, 132.0, 126.0, 125.8, 125.7, 115.1, 98.8, 54.6, 45.8, 45.4. HRMS (ESI): calcd for $C_{20}H_{19}N_3O$ $[M+H]^+$ 318.1601, found 318.1587. HPLC purity: 98.37%.

*5.1.4.2. 7-(2-(Diethylamino)ethyl)benzo[a]phenazin-5(7H)-one (**6a-2**).* Red solid, yield 43.1%. m.p. 169.1–171.2 °C. ^{1}H NMR (400 MHz, CD_3OD) δ 9.16 (d, *J* = 7.8 Hz, 1H), 8.37 (d, *J* = 8.5 Hz, 2H), 8.25 (d, *J* = 8.6 Hz, 1H), 8.06 (td, *J* = 7.2, 1.6 Hz, 1H), 7.95 (td, *J* = 7.2, 1.2 Hz, 1H), 7.89 (td, *J* = 7.2, 1.2 Hz, 1H), 7.84 (t, *J* = 7.2 Hz, 1H), 5.39–5.27 (m, 2H), 3.67–3.57 (m, 2H), 3.45 (q, J = 7.2 Hz, 4H), 1.40 (t, J = 7.3 Hz, 6H). ^{13}C NMR (101 MHz, CD_3OD) δ 182.8, 146.2, 140.2, 136.0, 133.3, 133.1, 132.8, 132.0, 131.9, 131.8, 125.9, 125.6, 125.6, 115.2, 98.8, 49.7, 48.4, 46.1, 12.2. HRMS (ESI): calcd for $C_{22}H_{23}N_3O$ $[M+H]^+$ 346.1914, found 346.1903. HPLC purity: 99.19%.

*5.1.4.3. 7-(2-Morpholinoethyl)benzo[a]phenazin-5(7H)-one (**6a-3**).* Red solid, yield 42.3%. m.p. 170.3–172.4 °C. ^{1}H NMR (400 MHz, CD_3OD) δ 8.98 (d, *J* = 7.9 Hz, 1H), 8.25 (d, *J* = 7.2 Hz, 1H), 8.16 (d, *J* = 8.1 Hz, 1H), 7.95 (d, *J* = 8.6 Hz, 1H), 7.88–7.75 (m, 3H), 7.62 (t, *J* = 7.6 Hz, 1H), 6.51 (s, 1H), 4.98 (s, 2H), 3.97 (s, 4H), 3.62–3.57 (m, 2H), 3.53 (s, 4H). ^{13}C NMR (101 MHz, DMSO-d_6) δ 180.4, 146.0, 138.9, 134.2, 132.3, 132.1, 131.4, 131.1, 130.9, 130.4, 124.7, 124.3, 114.5, 98.8, 63.4, 51.2, 49.1. HRMS (ESI): calcd for $C_{22}H_{21}N_3O_2$ $[M+H]^+$ 360.1707, found 360.1714. HPLC purity: 99.23%.

*5.1.4.4. 7-(2-(4-Methylpiperazin-1-yl)ethyl)benzo[a]phenazin-5(7H)-one (**6a-4**).* Red solid, yield 45.2%. m.p. 184.6–185.4 °C. ^{1}H NMR (400 MHz, $CDCl_3$) δ 8.95 (dd, *J* = 6.0, 3.3 Hz, 1H), 8.42 (dd, *J* = 6.0, 3.2 Hz, 1H), 8.06 (dd, *J* = 8.0, 1.4 Hz, 1H), 7.83–7.75 (m, 2H), 7.64 (td, *J* = 7.2, 1.6 Hz, 1H), 7.53 (d, *J* = 8.1 Hz, 1H), 7.44 (t, *J* = 7.5 Hz, 1H), 6.30 (s, 1H), 4.40 (t, *J* = 7.6 Hz, 2H), 2.86 (t, *J* = 7.6 Hz, 2H), 2.71 (s, 4H), 2.52 (s, 4H), 2.33 (s, 3H). ^{13}C NMR (101 MHz, CD_3OD) δ 183.0, 146.4, 140.4, 136.2, 133.4, 133.2, 132.9, 132.2, 132.1, 132.0, 131.9, 126.0, 125.7, 115.4, 98.9, 55.9, 54.0, 53.8, 46.0, 45.6. HRMS (ESI): calcd for $C_{23}H_{24}N_4O$ $[M+H]^+$ 373.2023, found 373.1998. HPLC purity: 97.57%.

*5.1.4.5. 7-(2-(Piperidin-1-yl)ethyl)benzo[a]phenazin-5(7H)-one (**6a-5**).* Red solid, yield 46.7%. m.p. 183.7–185.0 °C. ^{1}H NMR (400 MHz, CD_3OD) δ 8.67 (d, *J* = 7.7 Hz, 1H), 8.00 (d, *J* = 7.6 Hz, 1H), 7.86 (d, *J* = 7.6 Hz, 1H), 7.74 (d, *J* = 8.0 Hz, 1H), 7.67 (t, *J* = 7.3 Hz, 1H), 7.61 (t, *J* = 7.5 Hz, 1H), 7.54 (t, *J* = 7.1 Hz, 1H), 7.40 (t, *J* = 7.5 Hz, 1H), 6.14 (s, 1H), 3.41 (s, 2H), 3.21 (m, 6H), 1.92 (s, 4H), 1.68 (s, 2H). ^{13}C NMR (101 MHz, DMSO-d_6) δ 180.3, 146.0, 138.8, 134.2, 132.3, 132.0, 131.5, 131.4, 131.1, 130.9, 130.4, 124.6, 124.2, 114.5, 98.7, 52.3, 49.5, 49.3, 22.7, 21.5. HRMS (ESI): calcd for $C_{23}H_{23}N_3O$ $[M+H]^+$ 358.1914, found 358.1891. HPLC purity: 99.79%.

*5.1.4.6. 7-Propylbenzo[a]phenazin-5(7H)-one(**6a-6**).* Red solid, yield 48.2%. m.p. 158.9–160.3 °C. ^{1}H NMR (400 MHz, DMSO-d_6) δ 8.86–8.79 (m, 1H), 8.24–8.17 (m, 1H), 8.01 (dd, *J* = 8.0, 1.4 Hz, 1H), 7.88–7.79 (m, 3H), 7.73 (t, *J* = 7.1 Hz, 1H), 7.49 (t, *J* = 7.1 Hz, 1H), 6.22 (s, 1H), 4.33–4.24 (m, 2H), 1.85–1.75 (m, 2H), 1.11 (t, *J* = 7.4 Hz, 3H). ^{13}C NMR (101 MHz, DMSO-d_6) δ 179.6, 145.7, 138.7, 134.2, 132.4, 132.0, 131.4, 131.2, 130.8, 130.3, 124.6, 124.5, 124.0, 114.7, 98.1, 47.1, 18.6, 10.7. HRMS (ESI): calcd for $C_{19}H_{16}N_2O$ $[M+H]^+$ 289.1335, found 289.1332. HPLC purity: 99.39%.

*5.1.4.7. 7-(3-(Dimethylamino)propyl)benzo[a]phenazin-5(7H)-one (**6b-1**).* Red solid, yield 48.1%. m.p. 163.7–165.6 °C. ^{1}H NMR (400 MHz, $CDCl_3$) δ 9.02–8.87 (m, 1H), 8.44–8.34 (m, 1H), 8.04 (d, J = 7.9 Hz, 1H), 7.79–7.74 (m, 2H), 7.68–7.58 (m, 2H), 7.41 (t, J = 7.2 Hz, 1H), 6.29 (s, 1H), 4.34 (t, J = 8.0 Hz, 2H), 2.48 (t, J = 6.4 Hz, 2H), 2.34 (s, 6H), 2.12–1.97 (m, 2H). ^{13}C NMR (101 MHz, CD_3OD) δ 183.1, 146.4, 140.3, 136.3, 133.5, 133.2, 133.0, 132.0, 131.9, 126.0, 125.7, 115.3, 98.7, 57.1, 45.8, 45.6, 24.7. HRMS (ESI): calcd for $C_{19}H_{16}N_2O$ $[M+H]^+$ 332.1757, found 332.1740. HPLC purity: 99.34%.

*5.1.4.8. 7-(3-(Diethylamino)propyl)benzo[a]phenazin-5(7H)-one (**6b-2**).* Red solid, yield 43.9%. m.p. 163.1–164.5 °C. ^{1}H NMR (400 MHz, $CDCl_3$) δ 8.97–8.93 (m, 1H), 8.42–8.39 (m, 1H), 8.05 (dd, J = 8.0, 1.4 Hz, 1H), 7.79–7.75 (m, 2H), 7.65 (d, J = 7.6 Hz, 1H), 7.60 (td, J = 6.8, 1.6 Hz, 1H), 7.42 (td, J = 8.0, 1.6 Hz, 1H), 6.33 (s, 1H), 4.42–4.34 (m, 2H), 3.81 (t, J = 4.4 Hz, 4H), 2.53 (s, 6H), 2.14–2.02 (m, 2H), 1.58 (s, 2H). ^{13}C NMR (101 MHz, DMSO-d_6) δ 180.1, 145.9, 138.7, 134.2, 132.3, 131.9, 131.4, 131.3, 131.1, 130.9, 130.4, 124.6, 124.1, 114.4, 98.4, 63.3, 52.8, 51.2, 42.9, 19.9. HRMS (ESI): calcd for $C_{23}H_{25}N_3O$ $[M+H]^+$ 360.2070, found 360.2066. HPLC purity: 99.96%.

*5.1.4.9. 7-(3-Morpholinopropyl)benzo[a]phenazin-5(7H)-one (**6b-3**).* Red solid, yield 42.1%. m.p. 164.1–165.7 °C. ^{1}H NMR (400 MHz, $CDCl_3$) δ 8.97–8.93 (m, 1H), 8.42–8.37 (m, 1H), 8.05 (d, J = 8.0 Hz, 1H), 7.79–7.75 (m, 2H), 7.68–7.57 (m, 2H), 7.42 (t, J = 7.3 Hz, 1H), 6.33 (s, 1H), 4.40–4.34 (m, 2H), 3.81 (s, 4H), 2.53 (s, 6H), 2.11–2.05 (m, 2H). ^{13}C NMR (101 MHz, $CDCl_3$) δ 182.0, 146.8, 139.1, 135.0, 132.9, 132.1, 131.5, 131.3, 131.2, 131.1, 130.7, 125.3, 125.0, 123.8, 113.3, 99.0, 67.0, 55.3, 53.8, 44.2, 22.6. HRMS (ESI): calcd for $C_{23}H_{23}N_3O_2$ $[M+H]^+$ 374.1863, found 374.1864. HPLC purity: 99.77%.

*5.1.4.10. 7-(3-(4-Methylpiperazin-1-yl)propyl)benzo[a]phenazin-5(7H)-one (**6b-4**).* Red solid, yield 46.4%. m.p. 170.2–172.3 °C. ^{1}H NMR (400 MHz, $CDCl_3$) δ 9.00–8.92 (m, 1H), 8.42–8.38 (m, 1H), 8.05 (dd, J = 8.0, 1.2 Hz, 1H), 7.80–7.75 (m, 2H), 7.68–7.58 (m, 2H), 7.42 (td, J = 6.8, 1.6 Hz, 1H), 6.38 (s, 1H), 4.36 (t, J = 7.2 Hz, 2H), 2.61 (br, 8H), 4.53 (t, J = 6.4 Hz, 2H), 2.40 (s, 3H), 2.06 (m, 2H). ^{13}C NMR (101 MHz, CD_3OD) δ 183.0, 146.5, 140.4, 136.3, 133.6, 133.1, 133.0, 132.2, 132.1, 132.0, 131.9, 126.1, 125.7, 125.6, 115.5, 98.9, 55.9, 55.7, 53.8, 46.0, 45.7, 24.0. HRMS (ESI): calcd for $C_{24}H_{26}N_4O$ $[M+H]^+$ 387.2179, found 387.2177. HPLC purity: 99.66%.

*5.1.4.11. 7-(3-(Piperidin-1-yl)propyl)benzo[a]phenazin-5(7H)-one (**6b-5**).* Red solid, yield 43.5%. m.p. 163.5–165.4 °C. ^{1}H NMR (400 MHz, $CDCl_3$) δ 8.98–8.92 (m, 1H), 8.43–8.39 (m, 1H), 8.04 (dd, J = 8.0, 1.4 Hz, 1H), 7.82–7.71 (m, 3H), 7.62 (td, J = 7.2, 1.2 Hz,1H), 7.42 (td, J = 7.2, 1.2 Hz,1H), 6.30 (s, 1H), 4.35 (s, 2H), 2.49 (s, 6H), 2.08 (s, 2H), 1.70 (s, 4H), 1.51 (s, 2H). ^{13}C NMR (101 MHz, CD_3OD) δ 183.0, 146.4, 140.3, 136.2, 133.5, 133.1, 132.9, 132.1, 132.0, 131.8, 126.0, 125.7, 125.6, 115.4, 98.8, 56.6, 55.7, 45.9, 26.9, 25.3, 24.0. HRMS (ESI): calcd for $C_{24}H_{25}N_3O$ $[M+H]^+$ 372.2070, found 372.2076. HPLC purity: 98.38%.

*5.1.4.12. 7-(3-(Pyrrolidin-1-yl)propyl)benzo[a]phenazin-5(7H)-one (**6b-6**).* Red solid, yield 43.8%. m.p. 163.9–165.7 °C. ^{1}H NMR (400 MHz, CD_3OD) δ 8.41–8.33 (m, 1H), 7.88 (dd, J = 5.4, 3.2 Hz, 1H), 7.58 (d, J = 7.7 Hz, 1H), 7.46–7.33 (m, 4H), 7.18 (t, J = 6.9 Hz, 1H), 5.89 (s, 1H), 4.02 (s, 2H), 2.52 (t, J = 7.2 Hz, 2H), 2.47 (s, 2H), 1.86–1.76 (m, 2H), 1.72 (s, 4H). ^{13}C NMR (101 MHz, CD_3OD) δ 183.1, 146.5, 140.4, 136.3, 133.5, 133.2, 133.0, 132.1, 132.1, 131.9, 126.0, 125.7, 125.6, 115.4, 98.8, 55.1, 53.9, 45.8, 26.0, 24.4. HRMS (ESI): calcd for $C_{23}H_{23}N_3O$ $[M+H]^+$ 358.1914, found 358.1914. HPLC purity: 99.89%.

*5.1.4.13. 7-(4-(Dimethylamino)butyl)benzo[a]phenazin-5(7H)-one (**6c-1**).* Red solid, yield 46.5%. m.p. 150.3–152.5 °C. ^{1}H NMR (400 MHz, $CDCl_3$) δ 8.98–8.93 (m, 1H), 8.45–8.39 (m, 1H), 8.06 (d, J = 7.8 Hz, 1H), 7.81–7.75 (m, 2H), 7.64 (t, J = 7.2 Hz, 1H), 7.56 (d, J = 8.6 Hz, 1H), 7.43 (t, J = 7.6 Hz, 1H), 6.27 (s, 1H), 4.31–4.21 (m, 2H), 2.48 (t, J = 7.0 Hz, 2H), 2.35 (s, 6H), 2.03–1.90 (m, 2H), 1.83–1.73 (m, 2H). ^{13}C NMR (101 MHz, CD_3OD) δ 182.9, 146.2, 140.1, 136.1, 133.4, 133.2, 132.8, 132.0, 131.8, 131.8, 125.9, 125.6, 125.5, 115.3, 98.6, 59.9, 47.5, 45.5, 25.2, 24.6. HRMS (ESI): calcd for $C_{22}H_{23}N_3O$ $[M+H]^+$ 346.1914, found 346.1924. HPLC purity: 99.62%.

*5.1.4.14. 7-(4-(Diethylamino)butyl)benzo[a]phenazin-5(7H)-one (**6c-2**).* Red solid, yield 45.2%. m.p. 151.7–153.4 °C. ^{1}H NMR (400 MHz, $CDCl_3$) δ 8.97–8.93 (m, 1H), 8.43–8.40 (m, 1H), 8.04 (d, J = 7.4 Hz, 1H), 7.79–7.75 (m, 2H), 7.65–7.58 (m, 2H), 7.42 (dd, J = 7.2, 2.2 Hz, 1H), 6.27 (s, 1H), 4.29–4.21 (m, 2H), 2.67–2.52 (m, 6H), 2.00–1.86 (m, 2H), 1.81–1.65 (m, 2H), 1.09 (t, J = 7.1 Hz, 6H). ^{13}C NMR (101 MHz, CD_3OD) δ 183.0, 146.5, 140.3, 136.3, 133.5, 133.2, 133.0, 132.1, 132.0, 131.9, 126.0, 125.7, 125.6, 115.5, 98.7, 53.2, 47.7, 47.6, 24.8, 24.4, 11.4. HRMS (ESI): calcd for $C_{24}H_{27}N_3O$ $[M+H]^+$ 374.2227, found 374.2219. HPLC purity: 98.26%.

*5.1.4.15. 7-(3-(Dimethylamino)propyl)-3-methoxybenzo[a]phenazin-5(7H)-one (**6d-1**).* Red solid, yield 45.6%. m.p. 172.6–174.1 °C. ^{1}H NMR (400 MHz, $CDCl_3$) δ 8.88 (d, J = 8.7 Hz, 1H), 8.03 (d, J = 7.9 Hz, 1H), 7.84 (d, J = 2.3 Hz, 1H), 7.67 (d, J = 8.4 Hz, 1H), 7.61 (t, J = 7.6 Hz, 1H), 7.42 (t, J = 7.5 Hz, 1H), 7.31 (dd, J = 8.7, 2.4 Hz, 1H), 6.30 (s, 1H), 4.37 (s, 2H), 4.00 (s, 3H), 2.57–2.51 (m, 2H), 2.38 (s, 6H), 2.14–2.06 (m, 2H). ^{13}C NMR (101 MHz, DMSO-d_6) δ 179.5, 161.9, 145.4, 138.4, 134.5, 134.3, 131.2, 130.9, 130.0, 126.9, 124.6, 123.9, 118.8, 114.4, 106.7, 98.1, 55.6, 45.0, 43.9, 23.1. HRMS (ESI): calcd for $C_{22}H_{23}N_3O_2$ $[M+H]^+$ 362.1863, found 362.1867. HPLC purity: 99.75%.

*5.1.4.16. 7-(3-(Diethylamino)propyl)-3-methoxybenzo[a]phenazin-5(7H)-one (**6d-2**).* Red solid, yield 42.8%. m.p. 168.2–170.3 °C. ^{1}H NMR (400 MHz, $CDCl_3$) δ 8.88 (d, J = 8.8 Hz, 1H), 8.08 (d, J = 8.0 Hz, 1H), 8.03 (d, J = 8.4 Hz, 1H), 7.81 (t, J = 7.6 Hz, 1H), 7.70 (s, 1H), 7.57 (t, J = 7.5 Hz, 1H), 7.32 (d, J = 8.8 Hz, 1H), 6.99 (s, 1H), 4.56 (s, 2H), 3.93 (s, 3H), 3.50 (s, 2H), 2.45 (br, 4H), 1.39 (t, J = 6.9 Hz, 6H). ^{13}C NMR (101 MHz, CD_3OD) δ 181.7, 163.3, 145.4, 139.1, 136.5, 132.9, 131.8, 130.9, 128.1, 126.1, 125.7, 119.9, 117.5, 115.3, 107.1, 82.3, 56.0, 50.1, 44.8, 30.7, 22.0, 9.3. HRMS (ESI): calcd for $C_{24}H_{27}N_3O_2$ $[M+H]^+$ 390.2176, found 390.2163. HPLC purity: 98.73%.

*5.1.4.17. 7-(2-(Dimethylamino)ethyl)-3-methoxybenzo[a]phenazin-5(7H)-one (**6d-3**).* Red solid, yield 42.1%. m.p. 180.1–182.4 °C. ^{1}H NMR (400 MHz, CD_3OD) δ 9.16 (d, J = 9.0 Hz, 1H), 8.42 (d, J = 8.2 Hz, 1H), 8.31 (d, J = 8.7 Hz, 1H), 8.11 (t, J = 7.9 Hz, 1H), 7.92 (t, J = 7.6 Hz, 1H), 7.86 (d, J = 2.7 Hz, 1H), 7.59 (dd, J = 9.0, 2.7 Hz, 1H), 7.06 (s, 1H), 5.40–5.33 (m, 2H), 4.04 (s, 3H), 3.80–3.71 (m, 2H), 3.21 (s, 6H). ^{13}C NMR (101 MHz, CD_3OD) δ 182.6, 163.6, 146.0, 139.8, 136.4, 135.1, 132.6, 131.8, 131.5, 128.1, 126.0, 125.7, 120.0, 115.0, 107.6, 98.7, 56.0, 54.8, 45.9, 45.7. HRMS (ESI): calcd for $C_{21}H_{21}N_3O_2$ $[M+H]^+$ 348.1707, found 348.1712. HPLC purity: 97.87%.

*5.1.4.18. 7-(3-(Dimethylamino)propyl)-2-methoxybenzo[a]phenazin-5(7H)-one (**6d-4**).* Red solid, yield 44.6%. m.p. 160.2–161.8 °C. ^{1}H NMR (400 MHz, $CDCl_3$) δ 8.36 (d, J = 2.8 Hz, 1H), 8.31 (d, J = 8.8 Hz, 1H), 8.03 (d, J = 7.6 Hz, 1H), 7.68–7.60 (m, 2H), 7.40 (td, J = 7.6, 2.0 Hz, 1H), 7.29 (dd, J = 8.7, 2.7 Hz, 1H), 6.16 (s, 1H), 4.39–4.26 (m, 2H), 4.04 (s, 3H), 2.60 (s, 2H), 2.42 (s, 6H), 2.15–2.09 (m, 2H). ^{13}C NMR (101 MHz, CD_3OD) δ 189.4, 163.4, 145.5, 139.8, 137.00, 134.5, 132.4, 131.7, 127.4, 126.9, 119.9, 115.9, 108.7, 92.8, 81.9, 71.5, 56.3, 55.7, 45.3, 43.9, 30.7. HRMS (ESI): calcd for $C_{22}H_{23}N_3O_2$ $[M+H]^+$ 362.1863, found 362.1888. HPLC purity: 99.77%.

*5.1.4.19. 7-(3-(Dimethylamino)propyl)-10-methoxybenzo[a]phenazin-5(7H)-one (**6e-1**).* Red solid, yield 46.4%. m.p. 164.1–165.7 °C. ^{1}H NMR (400 MHz, D_2O) δ 7.62 (d, J = 7.1 Hz, 1H), 7.24 (d, J = 8.1 Hz, 1H), 7.18 (d, J = 9.5 Hz, 1H), 7.11–7.01 (m, 2H), 6.93 (dd, J = 9.3, 2.7 Hz, 1H), 6.49 (d, J = 2.6 Hz, 1H), 3.98 (s, 2H), 3.61 (s, 3H), 3.29–3.18 (m, 2H), 2.81 (s, 6H), 1.99–1.86 (m, 2H). ^{13}C NMR (101 MHz, D_2O) δ 174.7, 157.3, 142.3, 136.9, 135.9, 131.3, 130.9, 129.0, 128.3, 124.6, 124.1, 123.8, 123.5, 115.7, 109.8, 100.0, 55.9, 53.9, 44.8, 42.9, 21.5. HRMS (ESI): calcd for $C_{22}H_{23}N_3O_2$ $[M+H]^+$ 362.1863, found 362.1870. HPLC purity: 99.31%.

*5.1.4.20. 10-Chloro-7-(3-(dimethylamino)propyl)benzo[a]phenazin-5(7H)-one (**6e-2**).* Red solid, yield 42.6%. m.p. 173.0–174.8 °C. ^{1}H NMR (400 MHz, CD_3OD) δ 9.26 (d, J = 7.9 Hz, 1H), 8.51–8.45 (m, 2H), 8.37 (dd, J = 9.4, 1.5 Hz, 1H), 8.13–7.95 (m, 3H), 7.11 (s, 1H), 5.05–4.96 (m, 2H), 3.62–3.54 (m, 2H), 2.99 (s, 6H), 2.54–2.45 (m, 2H). ^{13}C NMR (101 MHz, DMSO-d_6) δ 179.1, 146.9, 138.5, 135.3, 131.7, 131.6, 131.2, 131.1, 130.0, 128.9, 128.3, 124.8, 124.5, 116.8, 98.5, 53.3, 43.6, 42.0, 20.4. HRMS (ESI): calcd for $C_{21}H_{20}N_3OCl$ $[M+H]^+$ 366.1368, found 366.1368. HPLC purity: 99.08%.

*5.1.4.21. 7-(3-(Dimethylamino)propyl)-9-methoxybenzo[a]phenazin-5(7H)-one (**6e-3**).* Red solid, yield 45.3%. m.p. 169.3–171.4 °C. ^{1}H NMR (400 MHz, CD_3OD) δ 9.28 (d, J = 8.1 Hz, 1H), 8.47 (d, J = 9.1 Hz, 2H), 8.06 (td, J = 7.2, 1.2 Hz, 1H), 7.98 (td, J = 7.2, 1.2 Hz, 1H), 7.74 (dd, J = 9.2, 2.4 Hz, 1H), 7.70 (d, J = 2.4 Hz, 1H), 7.48 (s, 1H), 5.27–5.16 (m, 2H), 4.27 (s, 3H), 3.67–3.62 (m, 2H), 2.99 (s, 6H), 2.61–2.50 (m, 2H). ^{13}C NMR (101 MHz, DMSO-d_6) δ 174.2, 164.0, 140.8, 138.0, 132.9, 132.6, 132.4, 131.3, 131.2, 130.8, 129.3, 124.4, 124.1, 117.1, 97.7, 97.0, 57.0, 53.4, 44.9, 42.1, 20.8. HRMS (ESI): calcd for $C_{22}H_{23}N_3O_2$ $[M+H]^+$ 362.1863, found 362.1858. HPLC purity: 98.63%.

*5.1.4.22. 7-(3-(Dimethylamino)propyl)-3,10-dimethoxybenzo[a]phenazin-5(7H)-one (**6f-1**).* Red solid, yield 44.8%. m.p. 172.3–173.5 °C. ^{1}H NMR (400 MHz, CD_3OD) δ 8.72 (d, J = 8.9 Hz, 1H), 7.90 (d, J = 9.3 Hz, 1H), 7.49–7.38 (m, 3H), 7.25 (dd, J = 8.9, 2.7 Hz, 1H), 4.63–4.57 (m, 2H), 3.95 (s, 3H), 3.85 (s, 3H), 3.49–3.42 (m, 2H), 2.93 (s, 6H), 2.36–2.23 (m, 2H). ^{13}C NMR (101 MHz, DMSO-d_6) δ 178.8, 161. 8, 155.8, 145.4, 137.5, 135.4, 134.3, 126.7, 124.9, 124.2, 120.5, 118.5, 115.6, 110. 8, 106.4, 96.9, 55.6, 55.4, 53.4, 43.2, 42.2, 20.6. HRMS (ESI): calcd for $C_{23}H_{25}N_3O_3$ $[M+H]^+$ 392.1969, found 392.1958. HPLC purity: 99.79%.

*5.1.4.23. 10-Chloro-7-(3-(dimethylamino)propyl)-3-methoxybenzo[a]phenazin-5(7H)- one (**6f-2**).* Red solid, yield 41.2%. m.p. 157.9–159.6 °C. ^{1}H NMR (400 MHz, DMSO-d_6) δ 8.72–8.66 (m, 1H), 7.97 (d, J = 6.3 Hz, 1H), 7.86 (d, J = 9.0 Hz, 1H), 7.72–7.67 (m, 1H), 7.60–7.55 (m, 1H), 7.42–7.34 (m, 1H), 6.35 (s, 1H), 4.34 (s, 2H), 3.93 (s, 3H), 3.36 (s, 2H), 2.81 (s, 6H), 2.18–2.06 (m, 2H). ^{13}C NMR (101 MHz, DMSO-d_6) δ 179.9, 162.2, 146.8, 138.0, 135.0, 134.4, 130.5, 129.7, 128.6, 127.6, 127.1, 124.3, 119.0, 116.2, 106.8, 98.8, 55.6, 53.5, 43.0, 42.3, 20.5. HRMS (ESI): calcd for $C_{22}H_{22}N_3O_2Cl$ $[M+H]^+$ 396.1473, found 396.1462. HPLC purity: 99.96%.

*5.1.4.24. 7-(3-(Dimethylamino)propyl)-3,9-dimethoxybenzo[a]phenazin-5(7H)-one (**6f-3**).* Red solid, yield 44.6%. m.p. 154.4–156.5 °C. ^{1}H NMR (400 MHz, CD_3OD) δ 8.88 (d, J = 8.9 Hz, 1H), 8.13 (d, J = 9.1 Hz, 1H), 7.65 (d, J = 2.6 Hz, 1H), 7.45–7.39 (m, 2H), 7.37 (d, J = 2.2 Hz, 1H), 4.82–4.76 (m, 2H), 4.15 (s, 3H), 3.98 (s, 3H), 3.60–3.51 (m, 2H), 2.99 (s, 6H), 2.47–2.38 (m, 2H). ^{13}C NMR (101 MHz, DMSO-d_6) δ 188.1, 162.4, 161.1, 141.0, 137.5, 134.6, 132.4, 131.9, 131.7, 130.5, 126.3, 124.5, 119.1, 114.3, 105.9, 97.3, 56.3, 55.4, 53.5, 43.5, 42.3, 20.5. HRMS (ESI): calcd for $C_{23}H_{25}N_3O_3$ $[M+H]^+$ 392.1969, found 392.1968. HPLC purity: 99.83%.

*5.1.4.25. 7-(3-(Dimethylamino)propyl)benzo[f]pyrido[2,3-b]quinoxalin-5(7H)-one (**6g-1**).* Red solid, yield 43.2%. m.p. 157.1–159.4 °C. ^{1}H NMR (400 MHz, $CDCl_3$) δ 8.96 (d, J = 7.0 Hz, 1H), 8.75 (s, 1H), 8.43–8.36 (m, 2H), 7.88–7.77 (m, 2H), 7.59–7.49 (m, 1H), 7.04 (s, 1H), 4.83 (s, 2H), 3.40 (s, 2H), 2.90 (s, 6H), 2.41 (s, 2H). ^{13}C NMR (101 MHz, CD_3OD) δ 183.8, 152.1, 148.3, 142.9, 141.4, 139.5, 133.3, 133.0, 132.7, 132.5, 131.2, 126.4, 125.9, 122.2, 100.7, 56.2, 43.6, 41.7, 22.6. HRMS (ESI): calcd for $C_{20}H_{20}N_4O$ $[M+H]^+$ 333.1710, found 333.1716. HPLC purity: 99.66%.

*5.1.4.26. 7-(3-(Piperidin-1-yl)propyl)benzo[f]pyrido[2,3-b]quinoxalin-5(7H)-one (**6g-2**).* Red solid, yield 42.1%. m.p. 156.4–158.2 °C. ^{1}H NMR (400 MHz, $CDCl_3$) δ 9.13–8.95 (m, 1H), 8.80 (dd, J = 4.5, 1.6 Hz, 1H), 8.51–8.39 (m, 2H), 7.95–7.80 (m, 2H), 7.59 (dd, J = 8.0, 4.5 Hz, 1H), 7.28 (s, 1H), 4.86 (s, 2H), 3.64 (d, J = 11.2 Hz, 2H), 3.42–3.31 (m, 2H), 2.73 (t, J = 12.2 Hz, 2H), 2.45 (s, 2H), 2.04–1.79 (m, 6H). ^{13}C NMR (101 MHz, CD_3OD) δ 183.5, 152.5, 148.0, 142.5, 141.2, 139.6, 133.2, 132.9, 132.7, 132.6, 131.0, 126.4, 125.9, 122.4, 100.7, 55.4, 54.5, 42.2, 24.3, 22.8, 22.0. HRMS (ESI): calcd for $C_{23}H_{24}N_4O$ $[M+H]^+$ 373.2023, found 373.2021. HPLC purity: 99.87%.

5.2. Topo I inhibitory activity

The effects of compounds on DNA relaxation catalyzed by DNA Topo I (TaKaRa, Kyoto, Japan) were determined by measuring the relaxation of supercoiled DNA pBR322 (TaKaRa, Kyoto, Japan) using camptothecin as a positive control. The reaction mixture was prepared according to the provided protocol, and incubated at 37 °C for 30 min. The reactions were terminated by the addition of dye solution containing 1% SDS, 0.02% bromophenol blue and 50% glycerol. The mixtures were applied to 1% agarose gel and subjected to electrophoresis for 1 h, in TAE buffer (40 mM Tris-acetate, 2 mM EDTA). Gels were stained for 30 min in 60 mL 1× TAE buffer with 2 μL Gel Red. DNA bands were visualized by transillumination with UV light and then photographed by Alpha Innotech digital imaging system.

5.3. Topo II inhibitory activity

We used the Topo II assay kit from TopoGEN to determine the effects of compounds on DNA relaxation catalyzed by *h*Topo II. Relaxation assays were carried out according to the manufacturer's instructions with minor modifications. The assay was performed in a final volume of 20 μL in Topo II reaction buffer (1× Topo II buffer = 50 mM Tris–HCl, pH 8.0, 150 mM NaCl, 10 mM $MgCl_2$, 2 mM ATP, 0.5 mM dithiothreitol, and 30 μg/mL BSA) with 0.2 μg pBR322 DNA. Compounds were included in the reactions at a constant solvent volume. Reactions were initiated by addition of 1U human Topo IIα, and incubated for 30 min at 37 °C. Reaction was terminated with 5× stop buffer (5 μL per 20 μL reaction volume). Stop buffer contained 5% sarkosyl, 0.0025% bromophenol blue and 25% glycerol. Reaction products were analyzed on a 1% agarose gel in TAE buffer (40 mM Tris-acetate, 2 mM EDTA). Gels were stained for 30 min in 60 mL 1× TAE buffer with 2 μL Gel Red DNA bands were visualized through transillumination with UV light and then photographed by Alpha Innotech digital imaging system.

5.4. Cell growth inhibition assay

The growth inhibitory effect of benzo[*a*]phenazin derivatives toward four different human cancer cell lines, including human promyelocytic leukemia cell line (HL-60), human chronic myelogenous leukemia cell (K562), cervical cancer cell line (HeLa), and adenocarcinomic human alveolar basal epithelial cell line (A549), were evaluated by using the MTT [3-(4,5-dimethylthiazol-2-yl)-

2,5-diphenyl-2H-tetrazolium-bromide] assay as described by Mosmann with minor modifications [26]. The cells were plated at a density of 1×10^4 per well in 96-well microplates, and allowed to incubate overnight. Benzo[*a*]phenazin derivatives were added to the wells at increasing concentrations (0–50 μM). After 48 h, each well was treated with 20 μL of 5 mg/mL MTT solution, and the cells were further incubated at 37 °C for 4 h. At the end of the incubation, the untransformed MTT was removed, and 150 μL DMSO was added. The microplates were well shaken to dissolve the formazan dye, and the absorbance at 570 nm was measured using a microplate-reader (Bio-Tek). All compound doses were parallel tested in triplicate, and the IC_{50} values were derived from the mean OD values of the triplicate tests versus compound concentration curves.

5.5. Topo I-mediated DNA cleavage assays

The assays were carried out as described previously with minor modification [16]. In brief, calf thymus Topo I (10 units), 0.1 μg negatively supercoiled pBR322 DNA, and 0.5–50 μM benzo[*a*]phenazin derivatives (or 0.1–50 μM camptothecin) were added in a total of 20 μL of Topo I buffer (50 mM Tris–HCl, pH 7.5, 50 mM KCl, 10 mM $MgCl_2$, 0.5 mM DTT, 0.1 mM EDTA, and 30 μg/mL bovine serum albumin). After incubating for 6 min at 37 °C to reach the cleavage/religation equilibrium, cleavage intermediates were trapped by adding 2 μL of 1% SDS, followed by 2 μL of 250 mM NaEDTA, pH 8.0. Proteinase K was added (2 μL of 0.8 mg/mL), and reactions were incubated for 30 min at 45 °C to digest the topoisomerase I. Samples were mixed with 2 μL of agarose gel loading buffer (30% sucrose, 0.5% bromophenol blue, and 0.5% xylene cyanole FF in 10 mM Tris–HCl, pH 7.9), heated at 70 °C for 2 min, and subjected to electrophoresis in a 1% agarose gel in TAE buffer (40 mM Tris-acetate, 2 mM EDTA) containing 0.5 μg/mL ethidium bromide. Cleavage was monitored with the conversion of negatively supercoiled plasmid to nicked DNA. DNA bands were visualized by using UV light, photographed by using Alpha Innotech digital imaging system, and quantitated with Image J software (NIH). The intensity of bands in the negative was proportional to the amount of DNA present.

5.6. ICE assays

The assays were carried out as described previously [33]. In brief, mid-log phase HL-60 cells were incubated with DMSO (vehicle, 1.0%, v/v), CPT (2, 5, and 10 μM), or benzo[*a*]phenazin derivatives (2, 5, and 10 μM) for 1 h. Cells were lysed with 1 mL of DNAzol (Invitrogen Life Technologies), and ethanol (0.5 mL, 100%) was then added and mixed with the lysate, and the solution was incubated overnight at −20 °C. The precipitated DNA was collected by centrifugation (13,000× g) at 25 °C for 10 min followed by washing twice with 75% ethanol and air drying. The DNA pellet was dissolved in 0.2 mL NaOH (8 mM) and then the pH was adjusted to 7.2 by HEPES (1 M, 25 mL). After centrifugation at 30,000× g for 10 min, the supernatant was used to quantify the DNA concentration. DNA (2 μg) dissolved to a final volume of 30 μL in NaH_2PO_4 buffer (25 mM, pH 6.5) was then loaded onto nitrocellulose membranes. Membranes were incubated overnight at 4 °C with rabbit monoclonal antibody to human Topo I (1:1000; Epitomics, USA) prepared as described previously [34], and then incubated for 1 h with human anti-rabbit secondary horseradish peroxidase-conjugated antibody (1:3000; Cell Signaling Technology, USA). Reactive bands were detected using SuperSignal West Pico chemiluminescent substrate (Thermo Scientific, USA), and chemiluminescence was exposed on Kodak X-Omat films.

5.7. Topo II-mediated DNA cleavage assays

The assays were carried out as described previously [16]. Briefly, 10 units of human Topo IIα, 0.1 μg negatively supercoiled pBR322 DNA, and 10–50 μM benzo[*a*]phenazin derivatives (or 100 μM VP-16) were added in a total of 20 μL Topo II buffer (50 mM Tris–HCl, pH 8.0, 150 mM NaCl, 10 mM $MgCl_2$, 2 mM ATP, 0.5 mM dithiothreitol, and 30 μg/mLBSA). Sample treatment (equilibrate, trapped, and digested) procedures were as described above. Cleavage was monitored with the conversion of negatively supercoiled DNA to linear molecules. Gel photography and quantitation of DNA bands were as described above.

5.8. ATPase domain related assays

The HsATPase plasmid and yeast strain, BCY123, for expressing human Topo II ATPase domain (HsATPase) were presented by Dr. Jian Ding from Shanghai Institute of Materia Medica. HsATPase was overexpressed and purified as described previously [34]. The ATP hydrolysis catalyzed by HsATPase was measured by using a non-isotopic malachite green assay. Briefly, a reagent containing malachite green (0.0812%, wt/vol), polyvinyl alcohol (2.32%, wt/vol), ammonium molybdate (5.72%, wt/vol, in 6 M HCl), and water mixed in a ratio of 2:1:1:2 was freshly prepared and kept at 4 °C. 100 mM ATP stock solution was freshly prepared in the assay buffer containing 100 mM Tris–HCl pH 7.4, 20 mM KCl, and 6 mM $MgCl_2$. A typical 25 μL reaction volume for measuring specific ATPase activity contained different concentrations of compounds. Reactions were started by the addition of 1 mM ATP, and incubated for 1 h at 37 °C, and terminated by the addition of 80 μL of malachite green reagent, and the absorbance was recorded at 620 nm on a microtiter plate reader (PowerWave XS2, Biotek). For kinetic studies, the same protocol was followed for increasing concentrations of ATP (250, 500, 800, 1,000, and 2000 μM) at each respective fixed concentration of compound 6f-3 (0, 5, 25, 50, and 100 μM) [9,35,36].

5.9. Topoisomerase I DNA unwinding assays

The ability of benzo[*a*]phenazin derivatives to unwind plasmid DNA was determined as described by John M. Fortune et al. [16,20] with modification. Relaxed pBR322 plasmid DNA utilized in unwinding assays was generated by treating negatively supercoiled pBR322 with topoisomerase I in topoisomerase I reaction buffer (50 mM Tris–HCl, pH 7.5, 50 mM KCl, 10 mM $MgCl_2$, 0.5 mM DTT, 0.1 mM EDTA, and 30 μg/mL bovine serum albumin) prior to the addition of other reaction components. Assay mixtures contained 0.1 μg relaxed pBR322 plasmid DNA, topoisomerase I (10 units), and compounds in 20 μL of topoisomerase I reaction buffer. Following a 10 min incubation of DNA and compound at room temperature, topoisomerase I was added, and reactions were incubated for 30 min at 37 °C. Reactions were stopped by adding an equal volume of phenol chloroform. Aqueous samples (20 μL) were removed from the reactions, and 3 μL of stop solution (0.77% SDS, 77 mM NaEDTA, pH 8.0) followed by 2 μL of agarose gel loading buffer (30% sucrose, in 10 mM Tris–HCl, pH 7.9) was added to each. Samples were subjected to electrophoresis in a 1% agarose gel in TAE buffer (40 mM Tris-acetate, 2 mM EDTA). DNA bands were stained with an aqueous solution of ethidium bromide (0.5 μg/mL), visualized with UV light, and photographed by Alpha Innotech digital imaging system.

5.10. UV–vis titration

Absorbance titration experiment was performed as previously described [16,37]. Binding assays were carried out in DPBS

(2.67 mM KCl, 1.47 mM KH_2PO_4, 138 mM NaCl, 8.06 mM Na_2HPO_4, pH 7.4). Solution of CT-DNA (Sigma–Aldrich) in DPBS gave a ratio of UV–vis absorbance of 1.8–1.9 at 260 and 280 nm, indicating that the DNA was sufficiently free of protein. The calf thymus DNA concentration was determined with UV absorbance at 260 nm using a molar absorptivity constant of 13,200 M $(bp)^{-1}$ cm^{-1}. Various compounds (15 μM) were prepared in DPBS with 1% DMSO in the presence or absence of increasing concentrations of CT-DNA (0–24 μM). Absorption spectra were recorded in the 400–600 nm spectral range after equilibration at room temperature for 5 min using UV–visible spectrophotometer UV-2450 (Shimadzu Instruments, Inc.).

5.11. Molecular docking

The structures of human Topo I and Topo IIα were generated base on their X-ray structures (PDB ID: 1K4T [38] and 1ZXM [39]) using SYBYL software package (Tripos, Inc. St. Louis, MO). The residues were corrected for physiological pH. In Topo IIα, Mg ion and its two binding water molecules were conserved. Molecular docking was carried out with Surflex-dock. For both proteins, the protomol that characterizes the binding site of the receptor were generated using a ligand-based approach. All other parameters accepted default settings. The docking results were visualized using the Discovery Studio software package.

Acknowledgments

We thank the Natural Science Foundation of China (91213302 and 21172272 for Z.-S. Huang, 21272288 for S.-L. Huang), the Guangdong Provincial Medicinal Research Foundation (A2011155 for S.-L. Huang), and Guangdong Provincial Key Laboratory of Construction Foundation (Grant 2011A060901014) for financial support of this study. We also thank Professor Jian Ding (State Key Laboratory of Drug Research, Shanghai Institute of Materia Medica, Chinese Academy of Sciences) for the plasmid gifts.

Appendix A. Supplementary data

Supplementary data related to this article can be found at http://dx.doi.org/10.1016/j.ejmech.2015.01.024.

References

[1] Y. Pommier, Drugging topoisomerases: lessons and challenges, ACS Chem. Biol. 8 (2013) 82–95.
[2] D.B. Khadka, W.J. Cho, Topoisomerase inhibitors as anticancer agents: a patent update, Expert. Opin. Ther. Pat. 23 (2013) 1033–1056.
[3] S. Salerno, F. Da Settimo, S. Taliani, F. Simorini, C. La Motta, G. Fornaciari, A.M. Marini, Recent advances in the development of dual topoisomerase I and II inhibitors as anticancer drugs, Curr. Med. Chem. 17 (2010) 4270–4290.
[4] C.L. Chen, F.L. Liu, C.C. Lee, T.C. Chen, W.W. Chang, J.H. Guh, A.A. Ahmed Ali, D.M. Chang, H.S. Huang, Ring fusion strategy for the synthesis of anthra[2,3-d] oxazole-2-thione-5,10-dione homologues as DNA topoisomerase inhibitors and as antitumor agents, Eur. J. Med. Chem. 87 (2014) 30–38.
[5] K.Y. Jun, H. Kwon, S.E. Park, E. Lee, R. Karki, P. Thapa, J.H. Lee, E.S. Lee, Y. Kwon, Discovery of dihydroxylated 2,4-diphenyl-6-thiophen-2-yl-pyridine as a non-intercalative DNA-binding topoisomerase II-specific catalytic inhibitor, Eur. J. Med. Chem. 80 (2014) 428–438.
[6] J.J. Perez, C.S. Lupala, P. Gomez-Gutierrez, Designing type II topoisomerase inhibitors: a molecular modeling approach, Curr. Top. Med. Chem. 14 (2014) 40–50.
[7] R. Karki, P. Thapa, H.Y. Yoo, T.M. Kadayat, P.H. Park, Y. Na, E. Lee, K.H. Jeon, W.J. Cho, H. Choi, Y. Kwon, E.S. Lee, Dihydroxylated 2,4,6-triphenyl pyridines: synthesis, topoisomerase I and II inhibitory activity, cytotoxicity, and structure-activity relationship study, Eur. J. Med. Chem. 49 (2012) 219–228.
[8] R. Karki, C. Park, K.Y. Jun, J.G. Jee, J.H. Lee, P. Thapa, T.M. Kadayat, Y. Kwon, E.S. Lee, Synthesis, antitumor activity, and structure-activity relationship study of trihydroxylated 2,4,6-triphenyl pyridines as potent and selective topoisomerase II inhibitors, Eur. J. Med. Chem. 84 (2014) 555–565.
[9] A.T. Baviskar, C. Madaan, R. Preet, P. Mohapatra, V. Jain, A. Agarwal, S.K. Guchhait, C.N. Kundu, U.C. Banerjee, P.V. Bharatam, N-fused imidazoles as novel anticancer agents that inhibit catalytic activity of topoisomerase IIalpha and induce apoptosis in G1/S phase, J. Med. Chem. 54 (2011) 5013–5030.
[10] J.T. Bau, Z. Kang, C.A. Austin, E.U. Kurz, Salicylate, a catalytic inhibitor of topoisomerase II, inhibits DNA cleavage and is selective for the alpha isoform, Mol. Pharmacol. 85 (2014) 198–207.
[11] M.Y. Kim, W. Duan, M. Gleason-Guzman, L.H. Hurley, Design, synthesis, and biological evaluation of a series of fluoroquinoanthroxazines with contrasting dual mechanisms of action against topoisomerase II and G-quadruplexes, J. Med. Chem. 46 (2003) 571–583.
[12] N. Vicker, L. Burgess, I.S. Chuckowree, R. Dodd, A.J. Folkes, D.J. Hardick, T.C. Hancox, W. Miller, J. Milton, S. Sohal, S. Wang, S.P. Wren, P.A. Charlton, W. Dangerfield, C. Liddle, P. Mistry, A.J. Stewart, W.A. Denny, Novel angular benzophenazines: dual topoisomerase I and topoisomerase II inhibitors as potential anticancer agents, J. Med. Chem. 45 (2002) 721–739.
[13] K.R. Hande, Topoisomerase II inhibitors, Update. Cancer Ther. 3 (2008) 13–26.
[14] G.J. Atwell, G.W. Rewcastle, B.C. Baguley, W.A. Denny, Potential antitumor agents. 50. In vivo solid-tumor activity of derivatives of N-[2-(dimethylamino) ethyl]acridine-4-carboxamide, J. Med. Chem. 30 (1987) 664–669.
[15] C.H. Nguyen, J.M. Lhoste, F. Lavelle, M.C. Bissery, E. Bisagni, Synthesis and antitumor activity of 1-[[(dialkylamino)alkyl]amino]-4-methyl-5H-pyrido [4,3-b]benzo[e]- and -benzo[g])indoles. A new class of antineoplastic agents, J. Med. Chem. 33 (1990) 1519–1528.
[16] J.M. Fortune, L. Velea, D.E. Graves, T. Utsugi, Y. Yamada, N. Osheroff, DNA topoisomerases as targets for the anticancer drug TAS-103: DNA interactions and topoisomerase catalytic inhibition, Biochemistry 38 (1999) 15580–15586.
[17] A.A. Adjei, M. Charron, E.K. Rowinsky, P.A. Svingen, J. Miller, J.M. Reid, J. Sebolt-Leopold, M.M. Ames, S.H. Kaufmann, Effect of pyrazoloacridine (NSC 366140) on DNA topoisomerases I and II, Clin. Cancer Res. 4 (1998) 683–691.
[18] D. Perrin, B. van Hille, J.M. Barret, A. Kruczynski, C. Etievant, T. Imbert, B.T. Hill, F 11782, a novel epipodophylloid non-intercalating dual catalytic inhibitor of topoisomerases I and II with an original mechanism of action, Biochem. Pharmacol. 59 (2000) 807–819.
[19] W.A. Denny, B.C. Baguley, Dual topoisomerase I/II inhibitors in cancer therapy, Curr. Top. Med. Chem. 3 (2003) 339–353.
[20] T. Yamagishi, S. Nakaike, T. Ikeda, H. Ikeya, S. Otomo, A novel antitumor compound, NC-190, induces topoisomerase II-dependent DNA cleavage and DNA fragmentation, Cancer Chemother. Pharm. 38 (1996) 29–34.
[21] M. Tarui, M. Doi, T. Ishida, M. Inoue, S. Nakaike, K. Kitamura, DNA-binding characterization of a novel anti-tumour benzo[a]phenazine derivative NC-182: spectroscopic and viscometric studies, Biochem. J. 304 (Pt 1) (1994) 271–279.
[22] P. Mistry, A.J. Stewart, W. Dangerfield, M. Baker, C. Liddle, D. Bootle, B. Kofler, D. Laurie, W.A. Denny, B. Baguley, P.A. Charlton, In vitro and in vivo characterization of XR11576, a novel, orally active, dual inhibitor of topoisomerase I and II, Anti Cancer Drug 13 (2002) 15–28.
[23] A.G. Jobson, E. Willmore, M.J. Tilby, P. Mistry, P. Charlton, C.A. Austin, Effect of phenazine compounds XR11576 and XR5944 on DNA topoisomerases, Cancer Chemother. Pharm. 63 (2009) 889–901.
[24] S.T. Zhuo, C.Y. Li, M.H. Hu, S.B. Chen, P.F. Yao, S.L. Huang, T.M. Ou, J.H. Tan, L.K. An, D. Li, L.Q. Gu, Z.S. Huang, Synthesis and biological evaluation of benzo [a]phenazine derivatives as a dual inhibitor of topoisomerase I and II, Org. Biomol. Chem. 11 (2013) 3989–4005.
[25] G.M. Rehberg, J.L. Rutherford, Synthesis of 5,7-dihydrobenzo[a]phenazin-5-one derivatives, J. Heterocycl. Chem. 32 (1995) 1643–1644.
[26] T. Mosmann, Rapid colorimetric assay for cellular growth and survival: application to proliferation and cytotoxicity assays, J. Immunol. Methods 65 (1983) 55–63.
[27] K.Y. Jun, E.Y. Lee, M.J. Jung, O.H. Lee, E.S. Lee, H.Y. Park Choo, Y. Na, Y. Kwon, Synthesis, biological evaluation, and molecular docking study of 3-(3′-heteroatom substituted-2′-hydroxy-1′-propyloxy) xanthone analogues as novel topoisomerase IIalpha catalytic inhibitor, Eur. J. Med. Chem. 46 (2011) 1964–1971.
[28] H. Huang, Q. Chen, X. Ku, L. Meng, L. Lin, X. Wang, C. Zhu, Y. Wang, Z. Chen, M. Li, H. Jiang, K. Chen, J. Ding, H. Liu, A series of alpha-heterocyclic carboxaldehyde thiosemicarbazones inhibit topoisomerase IIalpha catalytic activity, J. Med. Chem. 53 (2010) 3048–3064.
[29] D. Gurbani, V. Kukshal, J. Laubenthal, A. Kumar, A. Pandey, S. Tripathi, A. Arora, S.K. Jain, R. Ramachandran, D. Anderson, A. Dhawan, Mechanism of inhibition of the ATPase domain of human topoisomerase IIalpha by 1,4-benzoquinone, 1,2-naphthoquinone, 1,4-naphthoquinone, and 9,10-phenanthroquinone, Toxicol. Sci. 126 (2012) 372–390.
[30] J. Plsikova, L. Janovec, J. Koval, J. Ungvarsky, J. Mikes, R. Jendzelovsky, P. Fedorocko, J. Imrich, P. Kristian, J. Kasparkova, V. Brabec, M. Kozurkova, 3,6-bis(3-alkylguanidino)acridines as DNA-intercalating antitumor agents, Eur. J. Med. Chem. 57 (2012) 283–295.
[31] J.P. Malerich, T.J. Maimone, G.I. Elliott, D. Trauner, Biomimetic synthesis of antimalarial naphthoquinones, J. Am. Chem. Soc. 127 (2005) 6276–6283.
[32] D.R. Buckle, B.C. Cantello, H. Smith, R.J. Smith, B.A. Spicer, Synthesis and antiallergic activity of 2-hydroxy-3-nitro-1,4-naphthoquinones, J. Med. Chem. 20 (1977) 1059–1064.
[33] J.C. Yalowich, X. Wu, R. Zhang, R. Kanagasabai, M. Hornbaker, B.B. Hasinoff, The anticancer thiosemicarbazones Dp44mT and triapine lack inhibitory effects as catalytic inhibitors or poisons of DNA topoisomerase IIalpha, Biochem. Pharmacol. 84 (2012) 52–58.

[34] T. Hu, H. Sage, T.S. Hsieh, ATPase domain of eukaryotic DNA topoisomerase II. Inhibition of ATPase activity by the anti-cancer drug bisdioxopiperazine and ATP/ADP-induced dimerization, J. Biol. Chem. 277 (2002) 5944–5951.
[35] C.X. Hu, Z.L. Zuo, B. Xiong, J.G. Ma, M.Y. Geng, L.P. Lin, H.L. Jiang, J. Ding, Salvicine functions as novel topoisomerase II poison by binding to ATP pocket, Mol. Pharmacol. 70 (2006) 1593–1601.
[36] P. Daumar, B.M. Zeglis, N. Ramos, V. Divilov, K.K. Sevak, N. Pillarsetty, J.S. Lewis, Synthesis and evaluation of (18)F-labeled ATP competitive inhibitors of topoisomerase II as probes for imaging topoisomerase II expression, Eur. J. Med. Chem. 86 (2014) 769–781.
[37] G. Dong, S. Wang, Z. Miao, J. Yao, Y. Zhang, Z. Guo, W. Zhang, C. Sheng, New tricks for an old natural product: discovery of highly potent evodiamine derivatives as novel antitumor agents by systemic structure-activity relationship analysis and biological evaluations, J. Med. Chem. 55 (2012) 7593–7613.
[38] B.L. Staker, K. Hjerrild, M.D. Feese, C.A. Behnke, A.B. Burgin Jr., L. Stewart, The mechanism of topoisomerase I poisoning by a camptothecin analog, Proc. Natl. Acad. Sci. U. S. A. 99 (2002) 15387–15392.
[39] H. Wei, A.J. Ruthenburg, S.K. Bechis, G.L. Verdine, Nucleotide-dependent domain movement in the ATPase domain of a human type IIA DNA topoisomerase, J. Biol. Chem. 280 (2005) 37041–37047.